

DESIGN, MODELLING, AND FABRICATION OF INTERLACED THERMOPLASTIC COMPOSITES BY ADDITIVE MANUFACTURING

A Dissertation
Presented to
The Academic Faculty

by

Christopher M. Oberste

In Partial Fulfillment
of the Requirements for the Degree
Doctor of Philosophy in the
School of Materials Science and Engineering

Georgia Institute of Technology
August 2017

COPYRIGHT © 2017 BY CHRISTOPHER OBERSTE

DESIGN, MODELLING, AND FABRICATION OF INTERLACED THERMOPLASTIC COMPOSITES BY ADDITIVE MANUFACTURING

Approved by:

Dr. Ben Wang, Advisor
School of Industrial and Systems Eng.
School of Materials Science and Eng.
Georgia Institute of Technology

Dr. Kenneth Gall
Department of Mechanical Eng.
Duke University

Dr. Satish Kumar
School of Materials Science and Eng.
Georgia Institute of Technology

Dr. Robin K. Maskell
Chief Scientist
Solvay Composite Materials

Dr. Donggang Yao
School of Materials Science and Eng.
Georgia Institute of Technology

Date Approved: July 12, 2017

I would like to dedicate this dissertation to Coleen, whose encouragement and support
was essential to the success of this endeavor.

ACKNOWLEDGEMENTS

I would like to start by thanking my thesis advisor, Dr. Ben Wang, for his support and guidance throughout this project. He permitted me to embark on this adventure with only a few sketches in a notebook and graciously lent me his time when I needed assistance. I would also like to thank Dr. Donggang Yao for providing me with advice and guidance whenever I needed it.

I would like to acknowledge the Georgia Research Alliance for funding the construction of the WEAV3D prototype and the National Science Foundation for funding my customer discovery activities through the I-CORPS program (NSF 1643507). Furthermore, I would like to thank the Cytec Solvay Group's Cytec Doctoral Fellowship and Georgia Tech's President's Fellowship programs for providing me with financial support over the course of my graduate studies.

While the ultimate responsibility for design and development of the machines described in this thesis was my own, it would not have been possible without the support that I received from Georgia Tech staff. Many thanks to Phillip Cheng, Mike Jeffries, and Jonathan Holmes for the engineering expertise and insight they provided over the course of this project. I would also like to thank Ben Coffman, Chris Gilmore, Devin Brand, and the rest of the GTMI Prototyping Center for their continued patience and perseverance. I am indebted to Latanya Buckner, Martha Miller, Cheytoria Phillips, David Barnes, and the rest of the GTMI administrative staff for graciously offering their assistance in matters big and small.

I would like to thank Dr. Marie Thursby, Nicole Morris, and Margi Berbari for kindling my entrepreneurial spirit as part of the TI:GER program. I can honestly say that this program changed my life, and I am excited to see where my entrepreneurial adventures may take me. My TI:GER teammates, Daniel Ledesma, Lewis Motion, Nathan North, and Akshay Saxena, helped me realize the commercial potential of my technology and pushed me to grow as a person. To them, I owe a debt of gratitude.

Finally, I would like to express my profound gratitude to my parents and to my girlfriend for all of the support that they provided over my many years of study and research. They kept me motivated through hard times and kept me focused when life seemed full of distractions. I do not believe that I would have completed this thesis without them. Thank you.

TABLE OF CONTENTS

ACKNOWLEDGEMENTS	iv
LIST OF TABLES	viii
LIST OF FIGURES	ix
SUMMARY	xiii
CHAPTER 1. Introduction	1
1.1 Aerospace Challenges	1
1.2 Automotive Challenges	3
CHAPTER 2. Literature Review	5
2.1 Additive Manufacturing	5
2.2 Composite Structures	8
2.2.1 2D Laminated Composites	9
2.2.2 3D Composite Preforms	12
2.3 Composite Manufacturing	14
2.4 Composite Property Modelling	18
2.4.1 General Composite Theory	18
2.4.2 Mosaic Model	19
2.4.3 Fabric Geometry Model	21
2.4.4 Binary Model	25
2.4.5 Finite Element Analysis	26
2.4.6 Failure Models	28
CHAPTER 3. Design Methodology	30
3.1 Lean Manufacturing: Waste and Composite Manufacturing	30
3.1.1 Hand Lay-up	31
3.1.2 Resin Transfer Molding	34
3.1.3 Automated Tape Placement	35
3.1.4 Compression Molding	36
3.1.5 Generalization of Ideal Composite Forming Process	38
3.2 Design Theory	40
3.2.1 Elementary Steps of Composite Manufacturing	41
3.2.2 Design Axioms	44
3.2.3 Functional Requirements, Constraints, and Design Parameters	44
3.3 Synthesis	46
CHAPTER 4. Layer-By-Layer Manufacturing of Woven Composites: MAGIC	50
4.1 Concept	50
4.2 Implementation	54
4.3 Outcomes	59
4.4 Evaluation	59

CHAPTER 5. Continuous Composite Forming Machine: WEAV3D	63
5.1 Concept	63
5.2 Implementation	64
5.3 Outcomes	71
5.4 Composite Structures	74
5.5 Evaluation	76
CHAPTER 6. Modelling of Composite Properties	80
6.1 Concept	80
6.2 Implementation	81
6.3 Validation	89
CHAPTER 7. Contributions and Future Work	95
7.1 Contributions	95
7.2 Future Work	97
7.3 Commercialization	100
REFERENCES	101

LIST OF TABLES

Table 1	Comparison of composite forming processes	18
Table 2	Elementary Steps and Shaping Steps for Composite Manufacturing	42
Table 3	Print head position conversion table	87
Table 4	Comparison of moduli of traditional FGM and Volume Element FGM	91

LIST OF FIGURES

Figure 1	Diagram of stereolithography process [6]	6
Figure 2	Diagram of fused filament fabrication process [6]	6
Figure 3	Diagram of selective laser sintering process [6]	7
Figure 4	Tensile modulus (left) and tensile strength (right) of 2D laminates [2]	10
Figure 5	Diagram of unidirectional laminate [2]	10
Figure 6	Diagram of plain weave (left), twill (center), and satin (right) fabrics [16]	12
Figure 7	Diagram of orthogonal interlock fabric [18]	13
Figure 8	Diagram of through-thickness angle interlock fabric [18]	13
Figure 9	Diagram of layer-to-layer interlock fabric [18]	14
Figure 10	Schematic of automated tape placement [19]	15
Figure 11	Schematic of resin transfer molding [20]	16
Figure 12	Schematic of compression molding with sheet molding compound [21]	17
Figure 13	Representative element of the mosaic model [22]	20
Figure 14	Representative element of the 2D crimp model [26]	21
Figure 15	Macro-partitioning scheme of the partition model [31]	24
Figure 16	Micro-cell to combi-cell simplification of the partition model [32]	24
Figure 17	Binary model spring and rod approximation [35]	25
Figure 18	Diagram of iterative global/local FEA [37]	26
Figure 19	Comparison of real geometry vs. finite element geometry [38]	27
Figure 20	Steps of creating a finite element model [38]	28

Figure 21	Overview of design methodology	30
Figure 22	Hand lay-up value stream map	33
Figure 23	Resin transfer molding value stream map	34
Figure 24	Automated tape placement value stream map	36
Figure 25	Compression molding (SMC) value stream map	37
Figure 26	Compression molding (DLFT) value stream map	38
Figure 27	Ideal composite manufacturing process value stream map. Waste produced during the manufacturing process can be recycled and integrated into the composite during one of the processing steps	40
Figure 28	Mapping of Functional Requirements and Design Parameters. Market-specific functional requirements are on the left, lean functional requirements are on the right. Design parameters are shown in the middle and grouped by elementary steps. Colors are used to identify which design parameters are related to which FRs	48
Figure 29	MAGIC interlacing method. Pink and blue boxes represent the first and second warp head groups, respectively. The green box indicates the weft inserter. Colored lines show filaments deposited from the respective heads.	52
Figure 30	Method for forming plain weave structure. White boxes represent warp filaments, and belong to the 1 st or 2 nd warp group. Black boxes represent weft filaments. The deposition process starts at the upper left corner and proceeds down the left column, before continuing from the upper right column.	52
Figure 31	Weave transition, plain to twill to satin. Transition points are indicated.	53
Figure 32	Mock-up of MAGIC machine warp heads and roller. Mock-up enabled validation of weaving capability by sliding the warp heads into various positions.	54
Figure 33	Proof-of-concept of MAGIC machine warp rack	55
Figure 34	Proof-of-concept warp head. Note the discoloration around the linear shaft caused by lack of insulation between the heated and motion components.	56

Figure 35	Bench-scale prototype warp head, side view. This view is presented to emphasize the addition of the insulator and the redesigned heated component.	57
Figure 36	Bench-Scale prototype of MAGIC machine. This side view shows a single warp rack, print bed, and Z-stage. Inset A-A shows a close up view of the warp heads and the print bed.	58
Figure 37	MAGIC physical hierarchy and design parameters. Aerospace FR1: Reduce mass while maintaining or improving strength and stiffness. Aerospace Constraint 1: Maintain compatibility with conventional tooling for wing/fuselage panels. Aerospace Constraint 2: Utilize existing FAA-approved feedstock materials.	61
Figure 38	Diagram of WEAV3D machine. Left panel shows the side view of the machine. Filament spools shown in the left panel are warp filaments Right panel is a cutaway along Section A-A, showing the warp rack and weft inserter in detail. Filament spools shown in the right panel are weft filaments.	64
Figure 39	Mock-up of WEAV3D warp rack. Springs allow manual manipulation to explore the spatial relationship between the warp heads.	65
Figure 40	Front view of warp rack containing 10 warp heads. Warp filaments come out of the page.	66
Figure 41	Side view of a single warp head, color-coded.	67
Figure 42	CAD model of roller assembly	69
Figure 43	CAD model of weft inserter	70
Figure 44	WEAV3D machine, after warping	72
Figure 45	Close-up of WEAV3D shedding process.	72
Figure 46	Composite lattice, exiting hot roller. Machine feed direction is from left to right.	73
Figure 47	Finished composite lattice	73
Figure 48	Cross-section of 2D plain weave fabric geometry. Warp tapes (foreground and background) run from left to right. Weft tapes come out of page and are shaded black.	75

Figure 49	Cross-section of plain weave fabric geometry with single 3D interlace point (middle). Warp tapes (foreground and background) run from left to right. Weft tapes come out of page and are shaded black.	76
Figure 50	Cross-section of plain weave fabric geometry with partial 3D interlace point (middle). Warp tapes (foreground and background) run from left to right. Weft tapes come out of page and are shaded black.	76
Figure 51	WEAV3D Physical Hierarchy and Design Parameters	78
Figure 52	Illustration of how each of the four model components interact and the processes that occur within each component.	83
Figure 53	Woven partition (left) and head positions (right). Each red box represents a single volume element in the model.	84
Figure 54	Macro-element partition of four volume elements. Each red box represents one volume element. Within each box, the geometry is further partitioned into two warp (blue) and two weft (green) filaments. For structures that are not fully dense, the four corners of the box (shaded regions) are either represented as empty volume or filled with reinforced plastic.	86
Figure 55	Cell of interest is marked with an “X”. Adjacent cells are labeled “A1” through “A4”	87
Figure 56	2D geometric representation of volume elements. Each blue square represents one 10 mm by 10 mm element.	90
Figure 57	Free body diagram of boundary conditions. A 10 kN point load is applied to the lower-right volume element. It is assumed that the left side of the composite is fixed, while all remaining surfaces are free.	92
Figure 58	Deformed mesh after FEA analysis. The red boxes represent each volume element in the model, while the blue triangles show the mesh used for this test.	93
Figure 59	Graphical representation of flagged volume elements. A filled red box indicates that a particular volume element has exceeded the predetermined failure condition, in this case, the max strain parameter.	94
Figure 60	Proposed WEAV3D-injection molding process chain	98

SUMMARY

The aerospace and automotive industries both have incentives to improve fuel economy. The use of composite materials is a strategy that is being pursued in both industries. The current composite manufacturing value stream can be characterized as an assembly of batch processes, which results in limited design options, production inefficiency, and material waste. These limitations have prevented composites from achieving broad adoption, particularly in high-volume industries such as automotive manufacturing.

A method of design that combines a top-down definition of functional requirements with a bottom-up approach through the use of elementary steps was developed to address the composite material needs of the aerospace and automotive industries, while also integrating lean manufacturing into the total composite value chain. Using this methodology, two composite manufacturing processes were developed, one optimized for the automotive industry and one more appropriate for the aerospace industry. Prototype machines for each process were designed, constructed, and evaluated in the context of the specific functional requirements for each industry. These composite manufacturing processes enhance composite properties, reduce manufacturing costs and material waste, and increase production rate when compared to existing composite manufacturing processes. A model was developed to link machine parameters to macrostructural features in the final composite in order to predict mechanical behavior under specified load conditions. This model allows users to optimize composite structures and export print commands directly to the composite forming machine.

CHAPTER 1. INTRODUCTION

A composite material is a heterogeneous structure that consists of a combination of two or more different materials with significantly differing properties. Composites of natural materials have been used by humans since straw-reinforced mud bricks and wattle-and-daub structures were used to construct more resilient buildings in ancient times. There was very little additional development in composite materials until the early 1900s, when the newly developed Bakelite polymer was combined with natural fabrics to form a synthetic composite material. This structure found applications in mining helmets, aircraft propellers, and electrical insulation [1]. Despite this innovation, composites did not reach widespread use until after World War Two, when dramatic breakthroughs in both synthetic, engineered fibers and engineering-grade polymers finally enabled the creation of high-performance composites [2]. Today, high-performance composites are widely used in the aerospace, automotive, defense, and biomedical industries, where high specific strength and stiffness allow for the creation of strong, energy-efficient vehicles and devices. As part of the National Science Foundation's Innovation Corp program, over 100 interviews were conducted with individuals in a variety of industries to identify composites-related challenges and opportunities. These interviews allowed us to identify challenges specific to certain industries and direct our research efforts to create a useful product with commercial potential.

1.1 Aerospace Challenges

High performance composite materials used in the aerospace industry suffer from several deficiencies inherent to their manufacturing approach. Composite laminates made

from assemblages of two dimensional fabrics are prone to delamination, which results in poor impact resistance and damage tolerance. Composites formed from three dimensional composite preforms have sought to solve these issues; however, they are constrained by the cost and relative difficulty in making and working with a preform. In both instances, composite manufacturing methods limit the ability to manipulate fiber geometry and combine multiple materials into a single composite structure.

The aerospace industry was one of the earliest adopters of high-performance composites, as these materials offered a lightweight alternative to metallic structures, thus increasing carrying capacity and improving flight range. Unlike aluminum and steel, composites are not isotropic, which makes design of composite structures more difficult. While composite design has progressed significantly since the 1970s, many engineers still choose to treat carbon fiber composites as “black aluminum” by designing the composite to be quasi-isotropic. This simplifies the design process, but results in over-engineered structures that are not load-optimized. Furthermore, engineers are wary of delamination failure in structural composites, resulting in more over-engineering to compensate. All of this over-engineering adds weight to the composite, eroding its weight-saving potential and advantages over traditional materials.

The aerospace industry is constantly searching for materials and processes that will improve aircraft performance and reduce weight. In particular, optimization of existing materials has proven particularly promising as it allows the aircraft manufacturer to avoid the laborious and expensive process of qualifying completely new materials. Major advances in metal additive manufacturing have unlocked new design envelopes previously thought to be unattainable. This has once again reignited the competition

between metal and composites for structural applications. While composites can be optimized through the manipulation of plies within each layer, there is currently no way to optimize the macrostructure within the ply itself. As mentioned in the literature review below, most 2D laminates also suffer from very poor impact properties, which require the composite to be over-engineered to make it damage-tolerant. To enhance the capabilities of composites, it is necessary to unlock the composite macrostructure and enhance impact resistance.

Based on interviews with aerospace engineers in both the civilian and military sectors, there is a strong desire for better design tools to reduce the expertise required to design composite structures. Design tools would also enable the development of more complex composite structures, as structural validation costs are currently a significant barrier to innovation. In addition, the industry is heavily invested in research to mitigate and detect delamination failure. This dissertation presents a composite design tool and a composite manufacturing technology that allows the creation of delamination-resistant composite structures.

1.2 Automotive Challenges

The U.S. Environmental Protection Agency (EPA) and National Highway Traffic Safety Administration have issued final rules to reduce greenhouse gas emissions and improve vehicle fuel economy for model years 2017-2021, and have proposed rules for model years 2021-2025. Currently, the 2025 Corporate Average Fuel Economy (CAFE) target stands at 54.5 miles per gallon (mpg). Based on the EPA midterm review published in 2016, regulators project that automakers may only achieve an average fuel economy

between 50 and 52.6 mpg by 2025. Failure to meet the mandated target would trigger billions of dollars in fines. Ford, General Motors, and Fiat-Chrysler are particularly affected by the CAFE standards, due to their high-volume production of pickup trucks with low fuel economy. The automotive industry is desperately seeking technologies to help them meet the CAFE targets, especially through vehicle lightweighting. A 10% reduction in weight can boost fuel economy by 6-8%. While composites have a long history of use in the aerospace industry, current manufacturing technologies for continuous composites are too slow and expensive for use in automotive applications.

Traditional woven and unidirectional composite manufacturing technologies are an assembly of batch processes: fiber production, weaving, pre-impregnation of woven material with polymer (“prepregging”), and layup/consolidation. Layup tends to be a very labor-intensive process, contributing to the low throughput and high cost of most woven or unidirectional composites. This dissertation describes a manufacturing technology that combines two batch processes, weaving and consolidation, into a single continuous process that is completely automated, resulting in increased throughput and reduced process costs.

CHAPTER 2. LITERATURE REVIEW

The literature review for this dissertation can be divided into four distinct sections: additive manufacturing, composite structures, composite manufacturing, and composite property modelling. The additive manufacturing section discusses the history of additive manufacturing and key additive manufacturing principles that are applied in CHAPTER 4 and CHAPTER 5. The section on composite structures discusses the advantages and disadvantages of 2D laminates and 3D preform composites. Building on the first section, the composite manufacturing section describes the current state-of-the-art of composite manufacturing. Finally, the modelling section summarizes the large number of disparate approaches that have been used to model composite strength and elasticity in the past. These modelling methods will be used as a starting point for the model described in CHAPTER 6.

2.1 Additive Manufacturing

Additive manufacturing is the process of creating a finished part by depositing (adding) layer after layer of material, until the desired part is obtained [3]. While additive manufacturing is a broad term that encompasses many types of fabrication techniques, it is often used interchangeably with the term “3D printing” to describe the process of creating interdimensional objects. The earliest form of 3D printing was stereolithography (Figure 1), a process that commonly consists of a liquid photopolymer precursor that is polymerized at the surface of the fluid by patterned UV radiation [4]. By submerging the solidified polymer into the precursor, additional layers can be built upon the previous layers. The next major innovation in 3D printing was the development of fused filament fabrication (FFF) [5]. This process (Figure 2) involves melting a thermoplastic filament and depositing the molten material in thin layers. Compared to stereolithography, FFF

provides a greater variety of materials. Unfortunately, neither FFF nor stereolithography are well suited to fabricating structural components. Instead, these two printing methods have historically been used for prototyping.

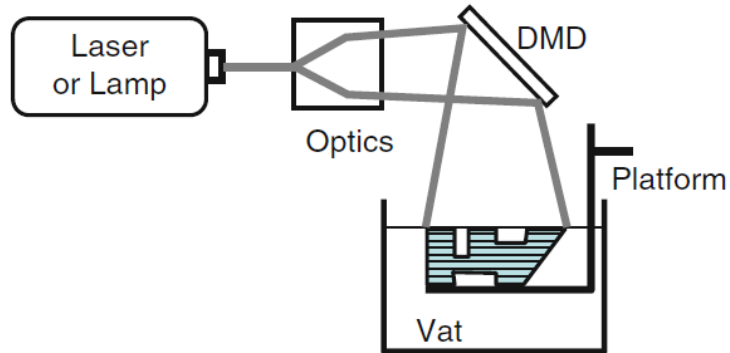


Figure 1: Diagram of stereolithography process [6]

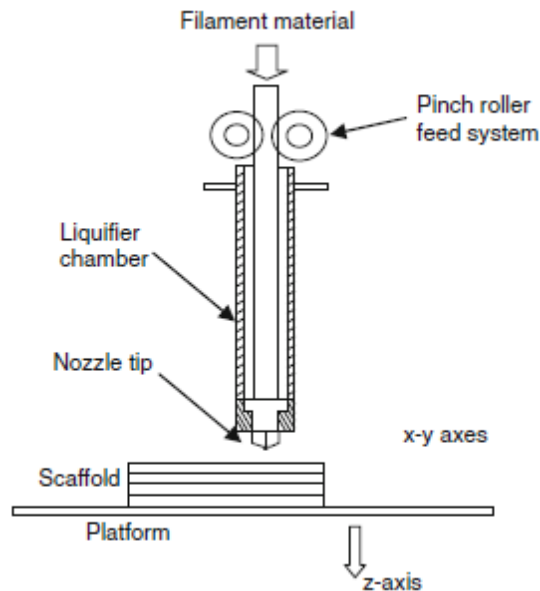


Figure 2: Diagram of fused filament fabrication process [6]

The first 3D printing system suitable for the fabrication of structural components was selective laser sintering (Figure 3) [7]. In this system, a thin layer of metal powder is deposited onto the print surface and a laser is used to selectively sinter the powder into a pattern. Another layer of powder is applied over the previously sintered layer, and the process is repeated, with the second layer being sintered to the first. While the components fabricated by this method are suitable for structural applications, metals are inherently higher density than polymers and composite structures.

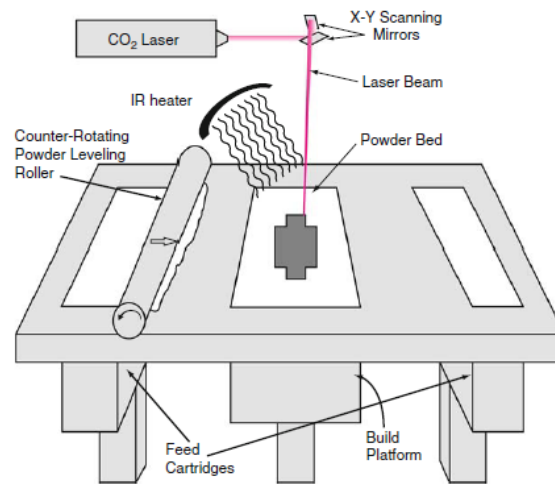


Figure 3: Diagram of selective laser sintering process [6]

Since the expiration of US patent 5,121,329 (Apparatus and method for creating three-dimensional objects) in 2009, various attempts have been made to adapt FFF printing to fabricate structural composites [5]. These attempts have largely focused on introducing reinforcement fibers into the polymer filament [8]. Oak Ridge National Laboratory has developed the Big Area Additive Manufacturing (BAAM) process, by combining a large FFF lay-down nozzle with an industrial scale gantry system. This allows for the rapid laydown of material over a large build area. Additionally, the large nozzle size allows chopped fibers to be incorporated into the filament [8]. This results in a marked improvement in stiffness; however, continuous fibers are needed for structural

applications. One company, Markforged (Cambridge, MA), has developed a continuous fiber reinforced filament for use with a modified FFF printer. This technology is able to form unidirectional (parallel and steered) composite structures [9]. Unfortunately, the fiber volume fraction in these composites is very low at 34.5% [10]. This limits the utility of these materials.

2.2 Composite Structures

The Engineering Dictionary defines a composite as “A combination of two or more materials (reinforcing elements, fillers, and composite matrix binder), differing in form of composition on a macroscale. The constituents retain their identities; that is, they do not dissolve or merge completely into one another although they act in concert. Normally, the components can be physically identified and exhibit an interface between one another...” [11]. While many types of composites exist, fiber-reinforced polymeric (FRP) composites are the most common type used in the aerospace and automotive industries, where they are valued for their high strength and low weight [2]. FRP composites consist of a fibrous structure embedded into a polymeric matrix. By themselves, the fibers used in the composite tend to have a very high specific strength and specific modulus when loaded in tension, but lack flexural rigidity and compressive strength. By combining the fibers with a polymeric matrix to “anchor” the fibers and transfer load between the fibers, the resulting composite can exhibit high specific strength and modulus when loaded in tension, compression, or flexure. In addition to being affected by the inherent mechanical properties of the fiber, the length scale of the fiber also has a strong effect on the composite’s final properties [12]. Both short-fiber reinforced polymeric (SFRP) composites and long-fiber reinforced polymeric (LFRP) composites consist of randomly oriented chopped fibers, ranging from millimeters to centimeters in length, respectively. This creates a quasi-isotropic material with no particular reinforcement bias. While this approach is often used to create coverings and

fairings, these kinds of FRP composites do not possess sufficient strength or toughness for structural applications. Continuous fiber-reinforced polymeric (CFRP) composites consist of filaments that run the entire length of the composite part. Compared to SFRP and LFRP composites, CFRP composites are significantly more expensive to produce, but with the advantage of much higher strength, stiffness, and toughness along the fiber direction. When continuous fibers are combined into interlaced (woven) fabric geometry, it is possible to reinforce the composite in several directions simultaneously [12].

2.2.1 2D Laminated Composites

Lamination involves uniting superimposed layers of material by adhesive. In a two-dimensional FRP composite laminate, the layers are made of woven or unidirectional textiles [12]. Many of these fabrication techniques make use of preimpregnated textiles (prepregs). These fabrics have been soaked or coated with resin prior to the laminate manufacturing process. Prepregs are easier to handle than dry textiles and have the additional benefit of enabling the formation of low porosity composites with controlled fiber volume fractions. Textiles that are not preimpregnated with resin are instead infused with resin during the consolidation process. Laminate structures exhibit good in-plane properties, but poor out of plane properties due to a lack of out-of-plane reinforcement (Figure 4). Furthermore, laminates are susceptible to impact damage, primarily in the form of delamination, due to a lack of mechanical linkage between the layers.

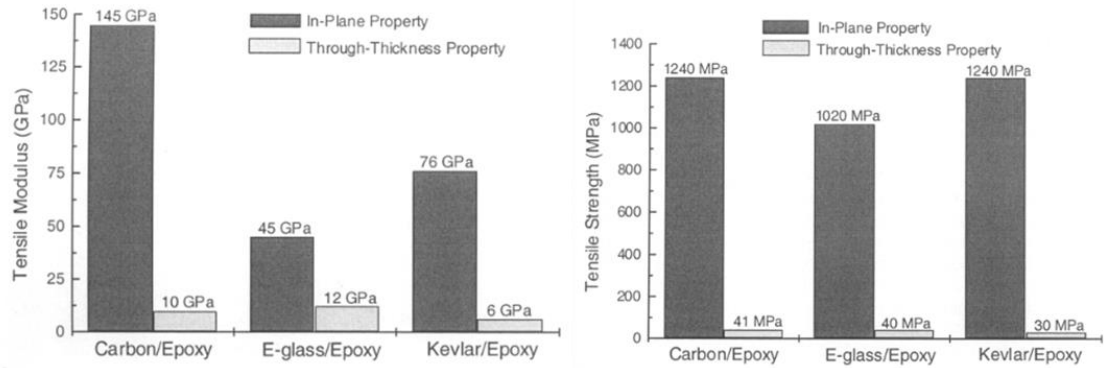


Figure 4: Tensile modulus (left) and tensile strength (right) of 2D laminates [2]

2D laminate properties are most strongly influenced by the choice of textile used for reinforcement [12, 13]. Two of the most common types of textiles are unidirectional and orthogonal textiles. Unidirectional textiles are assembled by aligning yarns together in parallel (Figure 5). Along the direction of yarn orientation, unidirectional textiles have the highest strength and stiffness of any textile, though their off-axis strength and stiffness are among the lowest, as adjacent yarns are not mechanically linked. Laminates can be assembled by stacking layers of unidirectional textiles, varying the axis of each layer to optimize composite properties [13].

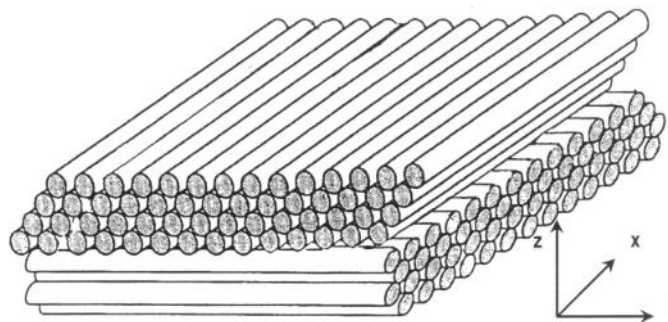


Figure 5: Diagram of unidirectional laminate [2]

A more balanced textile is created by the interlacing of orthogonally oriented yarns to create a woven structure. In orthogonal textiles, yarns that run the length of the fabric are termed warp yarns and those that run the width of the textile are termed weft yarns. The interlacing of the warp and weft yarns generates crimp, or curvature, in the yarns, which has an effect on the overall mechanical properties of the textile. Orthogonally woven structures can be classified by fabric geometry: plain weave, twill weave, and satin weave [14]. A plain weave is the simplest form of textile geometry, consisting of a repeat structure where the warp fiber passes over one weft yarn and under another weft yarn [15] (Figure 6). Plain weave fabrics have the lowest in-plane tensile stiffness and the highest in-plane shear stiffness of any orthogonal fabric geometry, due to the high degree of crimp [14]. Twill weave fabrics possess a repeat structure where the warp yarn passes over two or three weft yarns before passing under one, two, or three weft yarns [15]. This results in the formation of a very characteristic diagonal line (Figure 6). Twill weaves possess moderate in-plane tensile and shear stiffness [14]. The best textile structure for in-plane stiffness is the satin weave, due to the very low crimp inherent to these weaves [14]. In a satin weave, the warp yarns run over four or more weft yarns before interlacing with a weft yarn (Figure 6). While the low degree of crimp is good for in-plane stiffness, the lower level of interlacing between adjacent yarns translates to low in-plane shear strength [14]

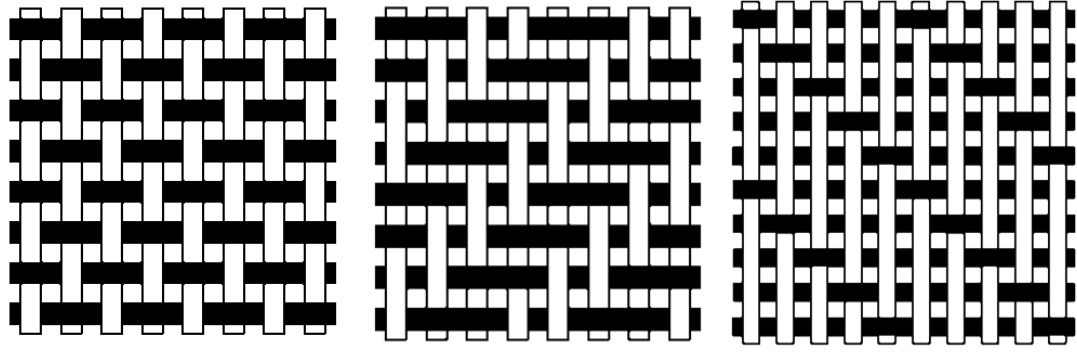


Figure 6: Diagram of plain weave (left), twill (center), and satin (right) fabrics [16]

2.2.2 3D Composite Preforms

Three-dimensional composites are created by infusing a three-dimensional textile preform with resin, usually during a resin transfer molding process [17]. Compared to 2D laminates, 3D composites are superior in terms of out-of-plane stiffness and impact resistance due to the inclusion of through-thickness yarns in the three-dimensional preform.

Three-dimensional textiles used in these composites can be classified into three distinct categories: orthogonal interlock fabrics, layer-to-layer angle interlock fabrics and through-thickness angle interlock fabrics [17, 18]. Orthogonal interlock fabrics consist of several layers of woven or $0^\circ/90^\circ$ alternating unidirectional textiles connected by through-thickness yarns that are orthogonal to the plane of the textile layers (Figure 7). Orthogonal interlock textiles provide excellent out-of-plane properties, but tend towards poor in-plane properties due to high crimp and reduced in-plane fiber volume fraction. Furthermore, the out-of-plane yarns are prone to buckling during the composite consolidation process, which can further degrade mechanical properties.

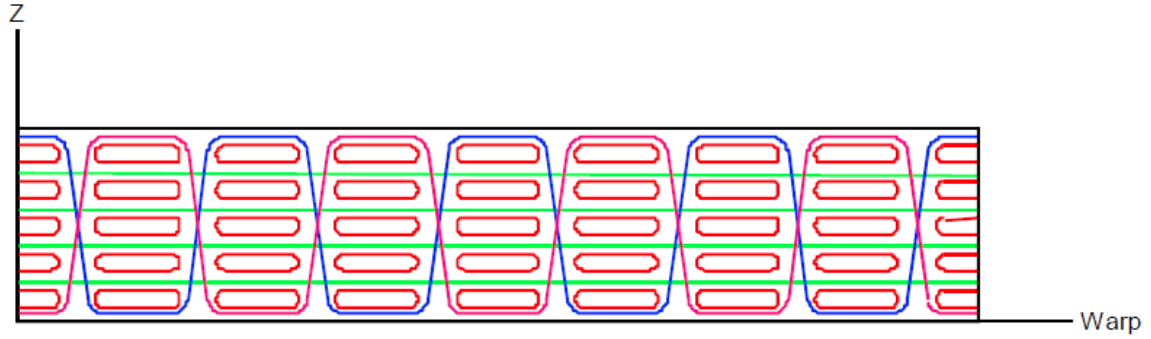


Figure 7: Diagram of orthogonal interlock fabric [18]

Through-thickness angle interlock textiles are similar to orthogonal interlock textiles in that they both contain yarns that pass through the full thickness of the fabric; however, in a through-thickness interlock structure these yarns are not orthogonal to the plane of each layer (Figure 8). This design has the benefit of increasing in-plane stiffness of the fabric and reducing crimp, but at the cost of reduced out-of-plane properties compared to orthogonal interlock textiles.

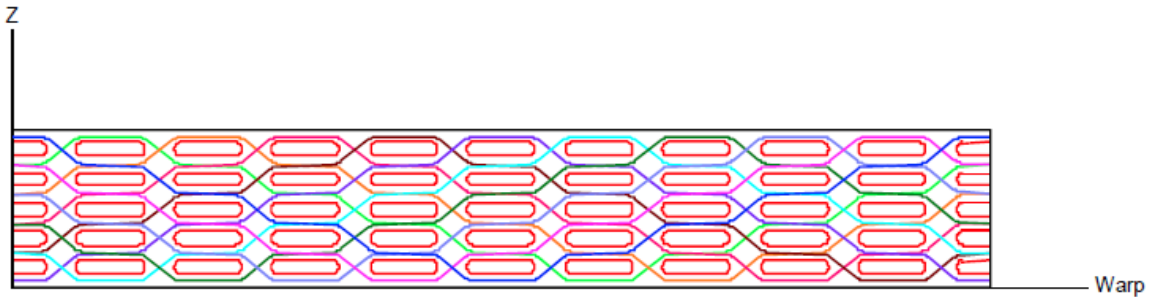


Figure 8: Diagram of through-thickness angle interlock fabric [18]

As seen in Figure 9, layer-to-layer interlock fabrics possess a structure that is very similar to that of a through-thickness angle interlock; however, the yarns in a through-thickness angle interlock only connect adjacent layers. The primary reason for utilizing this structure is to reduce delamination risk, which results in increased impact resistance

and compression strength. Because all three-dimensional textiles rely on alignment between adjacent layers in the textile to create an interlocking structure, it is not possible to insert in-plane, off-axis yarns to improve the in-plane shear strength of the textile.

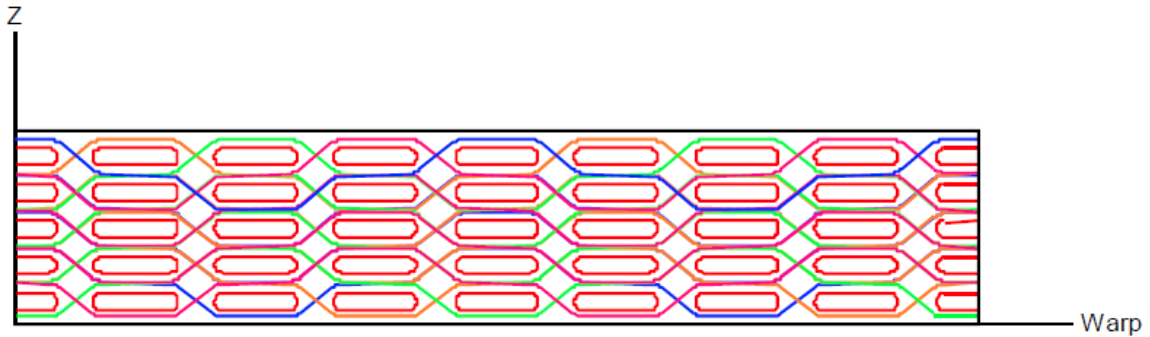


Figure 9: Diagram of layer-to-layer interlock fabric [18]

2.3 Composite Manufacturing

A variety of techniques are available to create laminated composites. Unidirectional composites are often manufactured through the use of automated tape placement or hand lay-up methods, while the interlaced nature of woven textiles makes them very easy to work with during hand lay-up, resin transfer molding, and compression molding processes. Hand lay-up is one of the simplest, but most labor-intensive, composite manufacturing techniques. In this technique, an operator applies layer after layer of dry or impregnated fabric to a mold, manually consolidating each layer as it is applied [2]. Once all layers have been applied, the uncured laminate is usually vacuum bagged to remove air and further consolidate the laminate. At this point it is cured either at room temperature or by the application of heat by an oven or autoclave process. This process has the advantage of being able to fabricate composites with very complex geometries, though the quality of the composite is entirely dependent on the skill of the

operator [17]. Automated tape placement is a highly precise process for creating composites from unidirectional prepreg textiles [19]. It can be thought of as a more advanced version of hand lay-up processes, where the human operator is replaced by a robot (Figure 10). This permits very precise fiber placement, though it can only be used on relatively simple curvilinear surfaces. Innovations in this field have focused on increasing laydown rate and the ability to steer fibers. This has led to the development of automated fiber placement, which replaces a single wide tape with several narrow overlapping tapes.

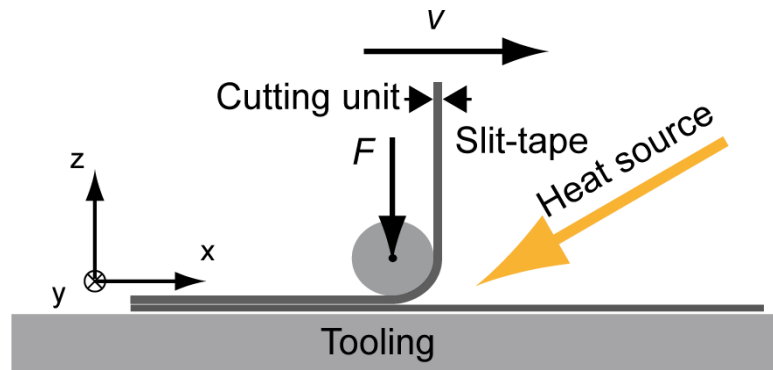


Figure 10: Schematic of automated tape placement [19]

Resin transfer molding (RTM) is a process in which a 2D or 3D textile preform is sealed into a closed mold and resin is pumped in to create the composite (Figure 11). This process is highly regarded in the composites industry, as it permits the formation of near net composites with low porosity and good consolidation [20]. This process is limited to certain industries due to the high cost of tooling. RTM molds require an upper and lower mold surface that must be capable of sealing; additionally, the mold must possess channels to pump in the resin and vent the air.

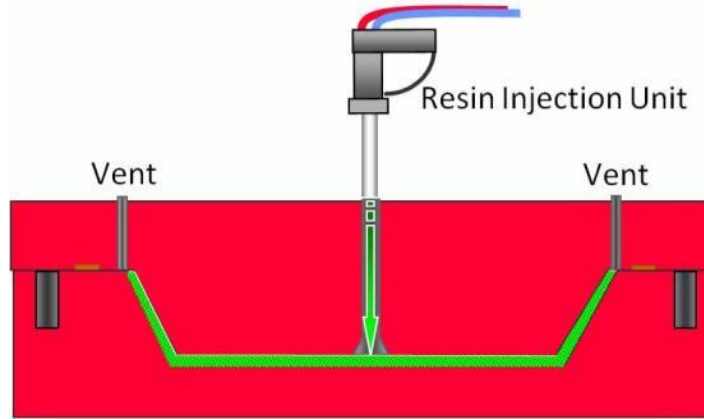


Figure 11: Schematic of resin transfer molding [20]

Compression molding is a technique that is mostly used to form thermoplastic composites, as it is capable of forming and cooling the resin matrix in a relatively short period of time (Figure 12). This process is generally used with unaligned long-fiber reinforcement, as the goal is to minimize cost [21]. Within the category of long-fiber reinforced compression molding, there are several types of molding precursor, including sheet molding compound (SMC), long fiber thermoplastics (LFT), and direct long-fiber thermoplastic molding (DLFT). SMC is a pre-compounded blend of fiber and thermoplastic resin that has been formed into a sheet. These sheets are generally heated in an oven before assembly in the mold. LFT also uses pre-compounded material, but formed into pellets instead of sheets. These pellets are fed into a single or twin-screw extruder, where they are melted and extruded into the mold cavity. In both of these examples, the fiber volume fraction depends on the content of the pre-compounded materials. In DLFT molding, compounding occurs during extrusion. This allows the manufacturer to control the fiber volume fraction and permits longer reinforcement fibers, which translate to better mechanical properties. Woven textiles can also be used with compression molding; however, they tend to suffer from fiber misalignment and

fiber damage caused by shear effects between the top and bottom mold during the forming process.

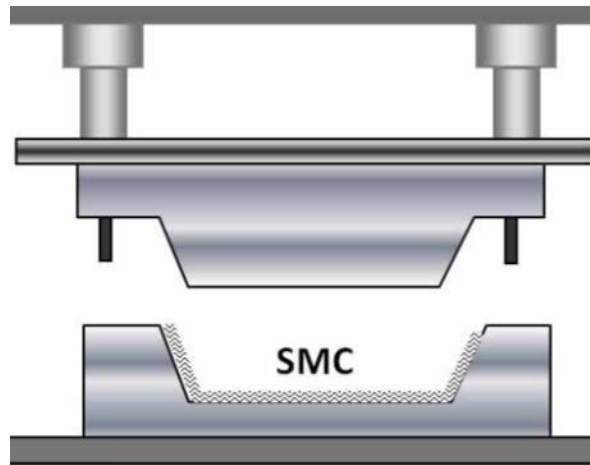


Figure 12: Schematic of compression molding with sheet molding compound [21]

Each of the previously described composite manufacturing processes comes with its own strengths and weaknesses and no single process is suitable for every possible application. Table 1 compares the relative production rate, touch labor, and capital cost for a number of composite forming processes. Processes used to make structural composites tend to have higher costs (through a combination of labor and capital) and lower production rates than non-structural composite forming processes.

Table 1: Comparison of composite forming processes

Structural Composites (Unidirectional or Woven)			
	Production Rate	Touch Labor	Capital Cost
Prepreg Hand Lay-up	Low	High	Low-Med
Automated Tape Laying	Med	Low	High
Resin Transfer Molding (RTM)	Med-High	Low-Med	Med-High
Non-Structural Composites (Long Fiber and Short Fiber)			
	Production Rate	Touch Labor	Capital Cost
Compression Molding (LFT/SMC)	High	Low	Low-Med
DLFT Molding	High	Low	Med-High
Injection Molding	High	Low	Med

2.4 Composite Property Modelling

2.4.1 General Composite Theory

Early composite material research examined how the addition of particulate or short reinforcement fibers changed the properties of a matrix from the pure state. While this dissertation is focused on woven-fabric reinforced composites, it is still important to mention prior work that modelled isotropic and unidirectional composite structures, as this is often used as a foundation for more complex woven-fabric models. Two of the most basic models are the rule of mixtures and the inverse rule of mixtures, which describe the theoretical upper and lower bounds, respectively, of the elastic modulus of a composite. As shown in Equation 1 and Equation 2, the rule of mixtures is a function of the modulus, E_i , of the constituent materials and the volume fraction, V_i , of each material with respect to the total volume of the composite. These equations can be proven through the use of isostress and isostrain assumptions [12]. In the isostress assumption, all the matrix and fiber components are considered to carry an equal stress. Under this

assumption, an inverse rule of mixtures relationship for stiffness can be derived. The isostrain assumption, which is more commonly used, assumes that the matrix and fiber will undergo strain during loading. This assumption results in the rule of mixtures equation for stiffness.

$$E_{composite} = V_f E_f + V_m E_m \quad (1)$$

$$\frac{1}{E_{composite}} = \frac{V_f}{E_f} + \frac{V_m}{E_m} \quad (2)$$

2.4.2 Mosaic Model

The mosaic model is one of the simplest models used to describe the elastic stiffness of woven-fabric reinforced composites. In the words of Ishikawa and Chou, “this model is idealized as an assemblage of asymmetrical cross-ply laminates” [22]. As shown in Figure 13, this results in a reduction of the interlacing of the fabric into planar tiles. By utilizing the classical laminated plate theory, the stiffness of these planar tiles can be calculated for the smallest repeat unit of the composite [22, 23]. The stiffness of this repeat unit is considered to be equivalent to the stiffness of the overall composite. This model was originally developed for plain-weave fabric-reinforced composites, where the mosaic structure would be a simple repeat of warp and weft plates; however, Ishikawa and Chou have also extended the model to cover satin weaves [22]. This modified mosaic model was termed the “bridging model”, as the interlaced regions are separated by a long bridge of fiber [22-24]. The model was able to identify that the bridge tiles carry more load than the tiles in the interlacing region. A one-dimensional mosaic

model has been used to provide an approximate solution to determine the mechanical properties of hybrid composites, or composites containing more than one type of reinforcement fiber [25].

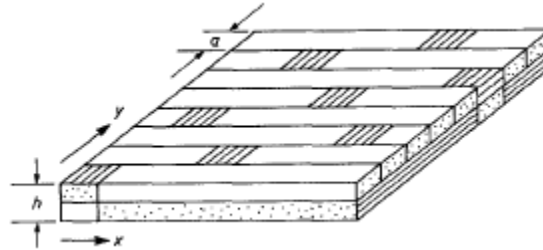


Figure 13: Representative element of the mosaic model [22]

One issue with the mosaic model is that it ignores the crimp in the yarns of the fabric structure, meaning that it disregards yarn undulation and the potential presence of gaps between yarns. Ishikawa and Chou initially proposed a 1D crimp model as a modification of their mosaic model, whereby the mosaic model was used to estimate properties in straight regions of the yarn, while classical laminated plate theory was used to model the undulated and pure matrix regions of the laminate [22, 23]. These separate components are then integrated along the warp direction to estimate the overall properties. While this is more accurate than the pure mosaic model, it still does not model crimp in the weft direction. Naik and Shembekar proposed a 2D crimp model to analyse 2D plain-weave laminates (Figure 14) [26]. This was achieved by recognizing that crimp in the warp direction is inversely proportional to crimp in the weft direction. In this model, the woven fabric was sliced into infinitesimal pieces, whose properties were calculated by classical laminated plate theory, before being assembled under isostrain or isostress conditions [26]. This model was further expanded to enable the analysis of a

multilayer laminate, with respect to alignment between the various laminas within the laminate [27, 28].

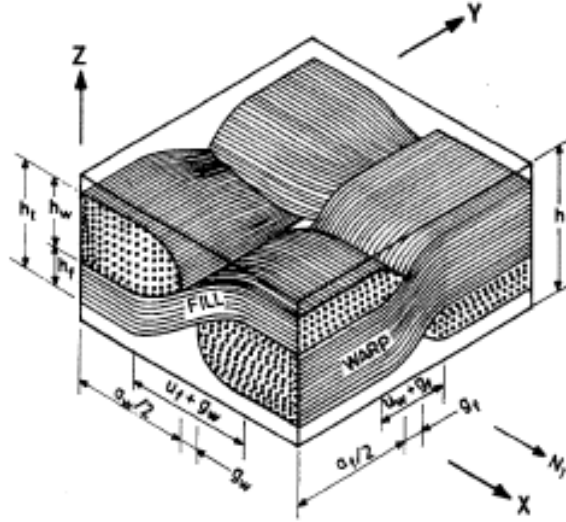


Figure 14: Representative element of the 2D crimp model [26]

2.4.3 Fabric Geometry Model

While not as accurate as finite element models, the fabric geometry model is useful in developing a relatively accurate model of elastic behaviour without the need for large amounts of computational power [13, 29-33]. The fabric geometry model considers the fiber and matrix in the composite as a collection of composite rods [29]. It relies on the stiffness-averaging method to generate a global stiffness tensor for the composite by averaging local stiffness tensors of each of the rods. These averages are weighted by the relative volume fraction of each rod. The fabric geometry model relies on two coordinate systems, the yarn coordinate system and the global coordinate system. Within the yarn coordinate system, yarns are aligned parallel to a single axis, usually designated axis 1, and the local stiffness tensor is calculated within this coordinate system. While this is

very convenient for determination of local stiffness tensors, in order to generate a global stiffness tensor all of these local stiffness tensors must be transformed from the yarn coordinate system to the global coordinate system. Equation 3 is the equation for transforming between coordinate systems and Equation 4 is the transformation tensor used, where l, m, and n are direction cosines that relate the yarn coordinate system to the global coordinate system [29]. The global stiffness tensor is shown in Equation 5, where it can be seen that by assuming orthotropy of the composite, the tensor can be reduced from 36 terms to 12 terms [33]. Because local stiffness tensors are averaged to create a global stiffness tensor, it is as easy to model heterogeneous fabric geometries as it is to model homogeneous ones.

$$C_{global} = T_{\epsilon}^T C_{local} T_{\epsilon} \quad (3)$$

$$T_{\epsilon} = \begin{matrix} l_1^2 & l_2^2 & l_3^2 & l_2 l_3 & l_1 l_3 & l_1 l_2 \\ m_1^2 & m_2^2 & m_3^2 & m_2 m_3 & m_1 m_3 & m_1 m_2 \\ n_1^2 & n_2^2 & n_3^2 & n_2 n_3 & n_1 n_3 & n_1 n_2 \\ 2m_1 n_1 & 2m_2 n_2 & 2m_3 n_3 & m_2 n_3 + m_3 n_2 & m_1 n_3 + m_3 n_1 & m_1 n_2 + m_2 n_1 \\ 2l_1 l_1 & 2l_2 l_2 & 2l_3 l_3 & l_2 n_3 + l_3 n_2 & l_1 n_3 + l_3 n_1 & l_1 n_2 + l_2 n_1 \\ 2l_1 m_1 & 2l_2 m_2 & 2l_3 m_3 & l_2 m_3 + l_3 m_2 & l_1 m_3 + l_3 m_1 & l_1 m_2 + l_2 m_1 \end{matrix} \quad (4)$$

$$C_{local} = S_{local}^{-1} = \begin{matrix} \frac{1}{E_1} & \frac{-\nu_{21}}{E_2} & \frac{-\nu_{31}}{E_3} & 0 & 0 & 0 \\ \frac{-\nu_{12}}{E_1} & \frac{1}{E_2} & \frac{-\nu_{32}}{E_3} & 0 & 0 & 0 \\ \frac{-\nu_{13}}{E_1} & \frac{-\nu_{23}}{E_2} & \frac{1}{E_3} & 0 & 0 & 0 \\ 0 & 0 & 0 & \frac{1}{G_{23}} & 0 & 0 \\ 0 & 0 & 0 & 0 & \frac{1}{G_{31}} & 0 \\ 0 & 0 & 0 & 0 & 0 & \frac{1}{G_{12}} \end{matrix} \quad (5)$$

One particular variation of the fabric geometry model is referred to as the “partition model.” This model involves reducing the fabric geometry model to a repeating unit cell, and then partitioning this cell into macro partitions [31, 32]. A plain-weave composite can be reduced to a unit cell containing two warp and two weft yarns, which after partitioning contains 16 partitions. An example of this macro partitioning scheme is shown in Figure 15. The purpose of this macro partitioning is to separate the yarns in the composite into discrete elements that can be further analysed. This is achieved by micro-partitioning each macro element, which allows straight and curved portions of the filament to be separated. The micro-cell is then converted into a combi-cell of the same volume fraction (Figure 16). Once it has been converted, the local stiffness matrix of the combi-cell can be determined through use of the classical laminated plate theory and application of isostress or isostrain conditions. The global stiffness matrix can then be calculated as previously described [32].

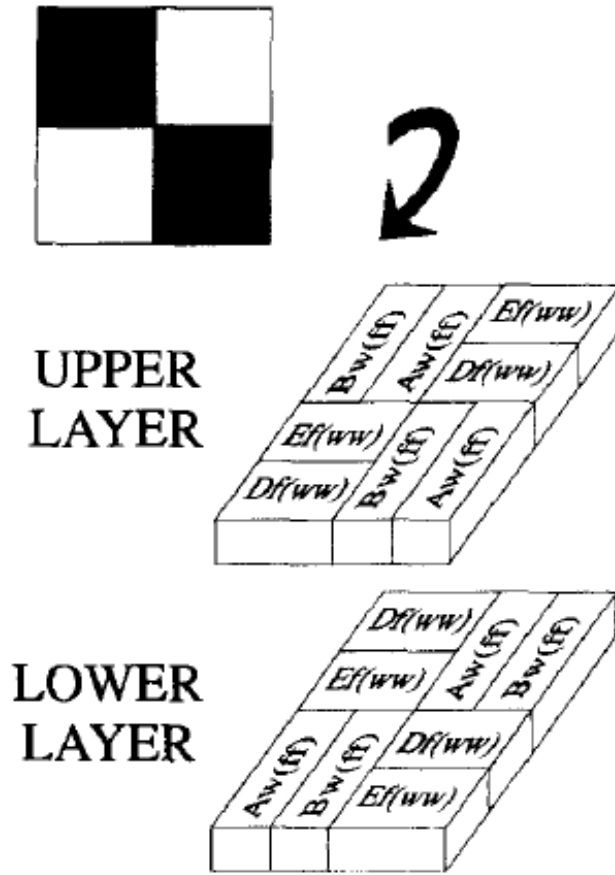


Figure 15: Macro-partitioning scheme of the partition model [31]

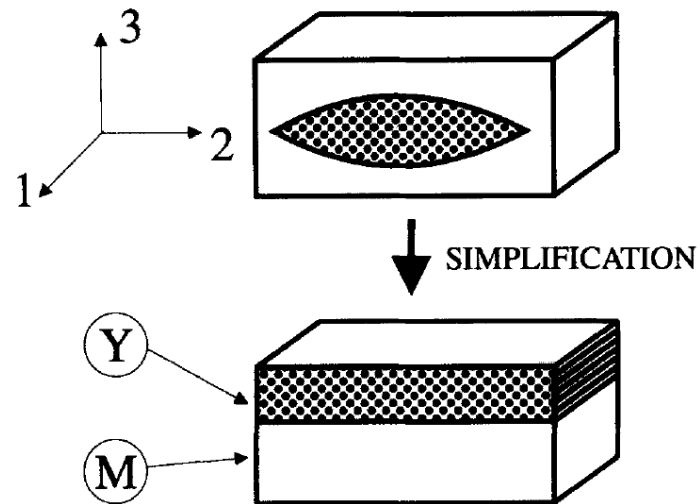


Figure 16: Micro-cell to combi-cell simplification of the partition model [32]

2.4.4 Binary Model

The binary model is a modelling approach used to describe the elastic behaviour of 3D woven composites. While other models, such as the orientation averaging model, rely on isostrain or isostress assumptions, the binary model instead considers the fabric to be an assemblage of rigid rods aligned along the axis of the yarn and an “effective medium” element. The rigid rods are used to model the axial properties of the yarns while the effective medium element models transverse stiffness, shear stiffness, and Poisson’s effect [34]. Warp weaver yarns are linked to the filler yarns by unidirectional springs (Figure 17). Elastic modulus, shear modulus, and Poisson’s ratio for the rigid rods, effective medium, and spring are modelled as approximations of variations on the values for a unidirectional tow. This appears to work well, as the majority of the composite properties are influenced by the tow elements, though it was identified that the predicted shear modulus can vary 10-30% from the experimental values. Initial application of the binary model was reserved for angle-interlock 3D woven structures; however, Stig and Hallstrom were able to adapt this model to adequately describe 3D orthogonal weave composites [35].

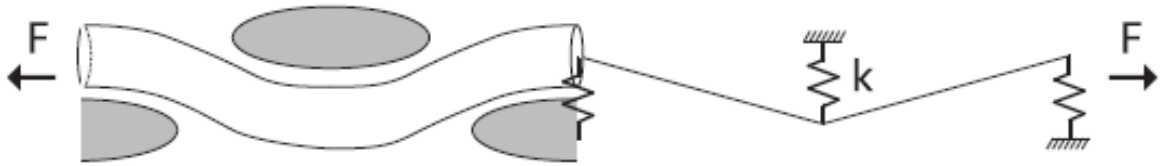


Figure 17: Binary model spring and rod approximation [35]

2.4.5 Finite Element Analysis

Finite element analysis (FEA) is considered the most accurate method of modelling composite properties; however, it is limited by the researcher's ability to geometrically model the fabric geometry and the availability of computer processing time. One type of FEA is the global/local FEA model [36, 37]. The mathematical approach used for this type of FEA is similar to that used by the fabric geometry model, as it relies on a relationship between the global stiffness tensor and the local stiffness tensor to determine the values of each. This is achieved by using an iterative approach consisting of a global and local model, whereby the global model is solved and the resulting strains are used as boundary conditions for the local model (Figure 18). If this does not result in convergence, the global strain value is modified and the process repeats itself until convergence is achieved. This global/local approach is used to increase computational efficiency of finite element analysis of composites.

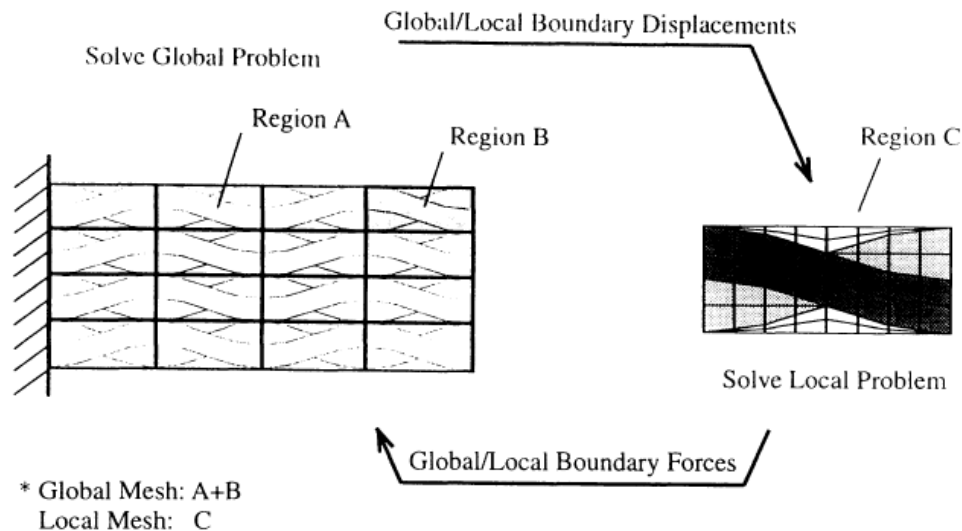


Figure 18: Diagram of iterative global/local FEA [37]

While early FEA required the use of simplified geometries due to software and computing limitations, modern FEA is capable of creating a model that is very faithful to the actual geometry of the composite (Figure 19). In this case, an accurate model of the geometry is created from a unit cell and appropriately meshed. Material properties are then assigned to the fiber and matrix regions of the unit cell and boundary conditions are assigned. The finite element analysis is then run and the stiffness or compliance matrix is extracted through manipulation of output data (Figure 20). Because the accuracy of the finite element model is dependent on the accuracy of the input geometry, this model works well for well-understood, homogeneous fabric geometries. To apply finite element modelling to heterogeneous fabric geometries, it would be necessary to create detailed unit cell models that geometrically describe the transition between every possible combination of fabric geometry.

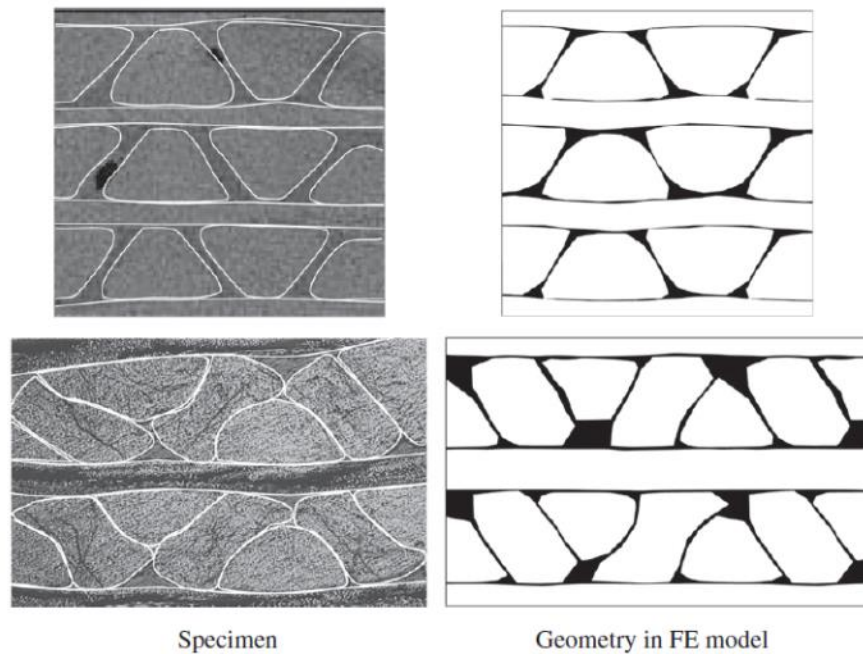


Figure 19: Comparison of real geometry vs. finite element geometry [38]

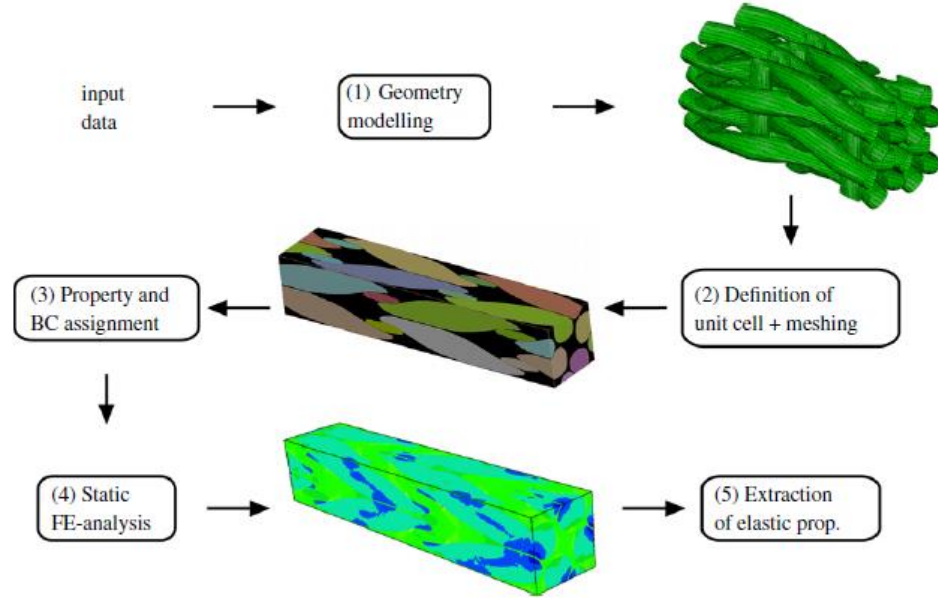


Figure 20: Steps of creating a finite element model [38]

2.4.6 Failure Models

In addition to the modelling of composite stiffness, modelling approaches can also be used to predict the failure strength of a composite. A wide range of potential failure models have been developed to describe both microscopic and macroscopic failure. Four models are described here, the maximum stress criterion, the maximum strain criterion, the Hill yield criterion, and the Tsai-Wu criterion. The maximum stress criterion is the simplest of the failure models, as it only requires comparing the maximum principal stress in the material's stress tensor against the uniaxial tensile strength of the material. If the maximum principal stress equals or exceeds the tensile strength, the material has failed [12]. Similarly, the maximum strain criterion determines that failure has occurred when principal strain in the material exceeds its allowable strain. These models work well on composites where the load is aligned with the yarn direction; however, they significantly underestimate shear load failure. A more accurate failure model was

developed by Rodney Hill [39, 40]. In this model, both principal and shear stresses are considered. The general form of the Hill yield criteria for an orthogonal structure is shown in Equation 6, where σ_i is defined as the normal stress in the “i-th” direction, σ_{iY} is the tensile yield stress in the “i-th” direction, τ_{12} is defined as the in-plane shear stress, and τ_{12Y} is the in-plane shear yield stress [12]. For a transversely isotropic structure, such as a unidirectional laminate or single-fiber model, Equation 6 can be reduced to Equation 7 [12]. It is important to note that the Hill yield criteria do not discriminate between tension and compression failure. The Tsai-Wu failure criterion was developed as a modification to the Hill yield criteria to compensate for its inability to address the disparity between tensile and compressive strength in most composites. The complete equations for the determination of all constants in the Tsai-Wu failure criterion are lengthy and complex, and as such, will not be described here. The key feature of the Tsai-Wu failure criterion is that it utilizes experimentally derived tensile strength, compressive strength, and equibiaxial tensile strength to generate the “F” constants depicted in Equation 8 [41]. By using the combination of failure strengths, this model predicts failure limits of a composite under a wide range of loading conditions [41].

$$\left(\frac{\sigma_1}{\sigma_{1Y}}\right)^2 + \left(\frac{\sigma_2}{\sigma_{2Y}}\right)^2 - \left(\frac{\sigma_1\sigma_2}{\sigma_{1Y}^2}\right) - \left(\frac{\sigma_1\sigma_2}{\sigma_{2Y}^2}\right) + \left(\frac{\sigma_1\sigma_2}{\sigma_{3Y}^2}\right) + \left(\frac{\tau_{12}}{\tau_{12Y}}\right)^2 = 1 \quad (6)$$

$$\left(\frac{\sigma_1}{\sigma_{1Y}}\right)^2 + \left(\frac{\sigma_2}{\sigma_{2Y}}\right)^2 - \left(\frac{\sigma_1\sigma_2}{\sigma_{1Y}^2}\right) + \left(\frac{\tau_{12}}{\tau_{12Y}}\right)^2 = 1 \quad (7)$$

$$\begin{aligned} &F_1\sigma_1 + F_2\sigma_2 + F_3\sigma_3 + F_4\sigma_4 + F_5\sigma_5 + F_6\sigma_6 + F_{11}\sigma_1^2 + F_{22}\sigma_2^2 + F_{33}\sigma_3^2 + \\ &F_{44}\sigma_4^2 + F_{55}\sigma_5^2 + F_{66}\sigma_6^2 + 2F_{12}\sigma_1\sigma_2 + 2F_{13}\sigma_1\sigma_3 + 2F_{23}\sigma_2\sigma_3 \leq 1 \end{aligned} \quad (8)$$

CHAPTER 3. DESIGN METHODOLOGY

A method of design (Figure 21) that combines a top-down definition of functional requirements with a bottom-up approach through the use of elementary steps was developed to address the composite material needs of the aerospace and automotive industries, while also integrating lean manufacturing into the total composite value chain.

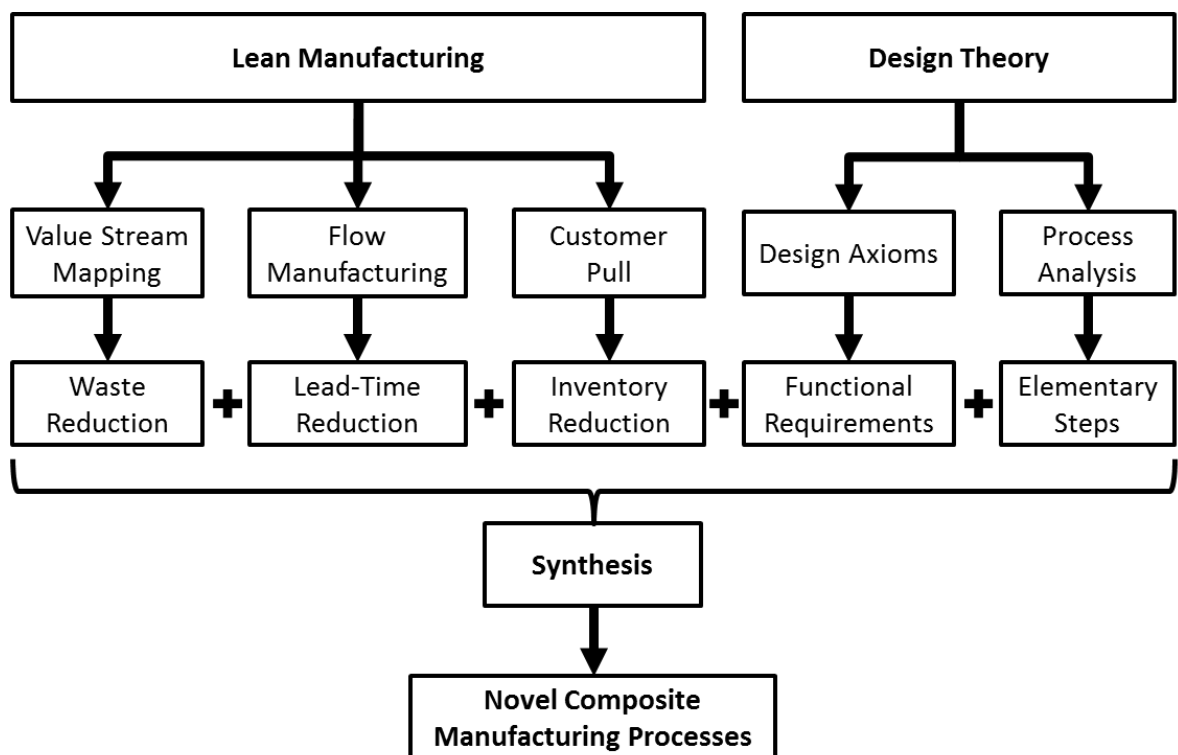


Figure 21: Overview of design methodology

3.1 Lean Manufacturing: Waste and Composite Manufacturing

Lean manufacturing was first developed by Toyota as a way to reduce waste in the production process. Waste in lean manufacturing is broadly defined, encompassing everything from unproductive work schedules to excessive inventory. Full

implementation of lean manufacturing principles results in reduced cycle time, reduced inventory, increased productivity (throughput), and better capital utilization [42]. The concept of lean manufacturing is well established in the composite industry; however, most lean efforts focus on reducing waste within the bounds of their existing manufacturing processes. This is problematic, as the composite manufacturing supply chain is heavily dependent on batch processing, which forces suppliers to build inventory to compensate for imbalanced customer demand.

Value stream mapping is a lean manufacturing tool used to visualize manufacturing flow at the system level. In order to examine the inefficiencies that exist in the current composite manufacturing supply chain, value stream maps have been constructed for each of the four major composite forming processes: hand lay-up, resin transfer molding, automated tape placement, and compression molding (SMC and DLFT). Each value stream map starts with fiber feedstock, ends with the composite part, and is grouped by supplier. The value stream maps (Figure 22 to Figure 27) are simplified from the form traditionally used in lean manufacturing methodology in order to emphasize key processes and waste areas. As such, some process steps are omitted or abbreviated. For each map, purple boxes indicate feedstock coming from a supplier, blue boxes indicate processing steps, green boxes indicate the product, and red boxes indicate waste.

3.1.1 Hand Lay-up

Hand-layup for aerospace applications utilizes woven and/or unidirectional prepreg material (Figure 22). Fibers are converted into woven fabrics by a weaving company and the dry fabrics are impregnated with resin by a prepregging company before being sent to

a composite manufacturer for lay-up and curing. In addition to manufacturing defects, there are numerous sources of waste that are directly related to the supply chain. Weaving companies are required to offer a catalog of fabrics with different fiber types, yarn denier, and weave patterns. Setting up a new fabric for weaving is a time consuming process that can take days and as a result, weaving companies tend to run large batches of fabric, even if it is an uncommon order. This results in excess inventory, which must be managed and kept in good condition. Most orders range from hundreds of yards to one or more full rolls. For orders of less than one full roll, the weaving company will measure and cut the customer's order from a full roll. This can result in so-called end rolls, which cannot be sold as they contain less one order's worth of material. This material must be discarded or donated to clear inventory space.

Prepregging represents another opportunity to generate waste, in the form of expired prepreg. This form of waste usually only occurs with prepregs that use thermoset resins, as thermoplastics tend to be shelf-stable at room temperature. Much like the weaving company, prepregging companies tend to batch produce their material as they must clean and reset the production line every time they change from one resin to another. In order to delay the resin curing process, prepregs are kept in freezers; however, even in this condition, most prepregs will expire within one year. This is particularly problematic, since the prepreg manufacturer must guarantee a minimum shelf life to their customer, the composite manufacturer. Waste generated at the composite manufacturer tends to be the most expensive, as the material has acquired significant value after passing through the previous two suppliers. The first major source of waste occurs when the composite manufacturer converts rolls of prepreg into plies that can be used for layup. A great deal

of effort is made to nest plies in order to minimize waste at this step; however, it is not possible to eliminate waste entirely due to the irregular shape of most plies. Additional waste is generated during the composite trim process, where the unfinished, cured composite is trimmed to its final dimensions. Beyond material waste, the hand lay-up process is very labor intensive, and composite parts are often batch-cured in large autoclaves, which adds additional cost and time.

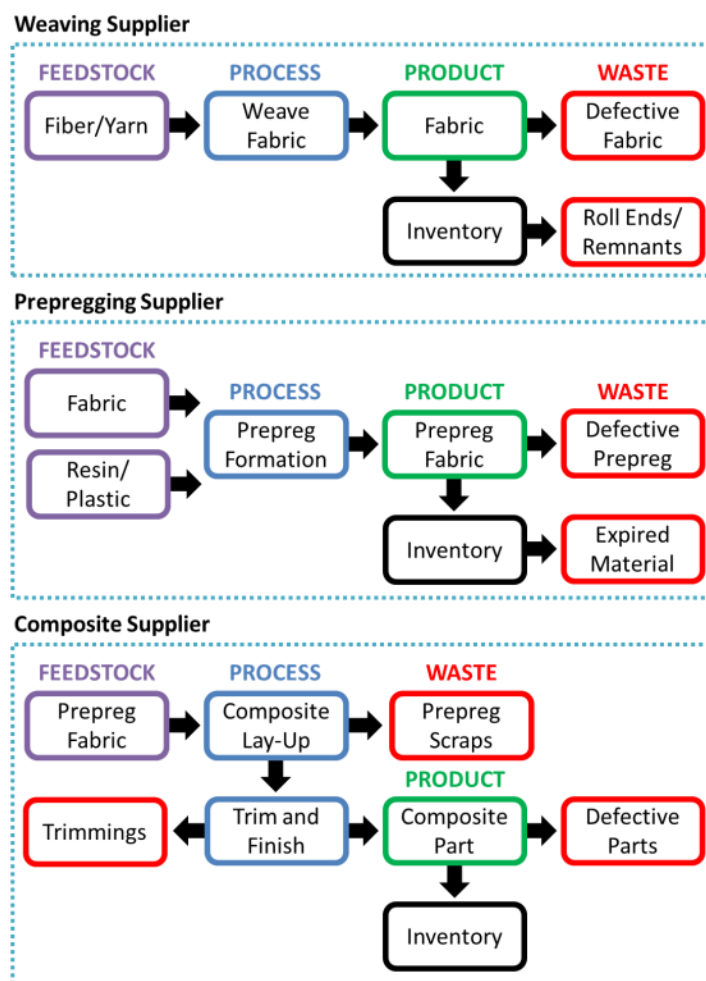


Figure 22: Hand lay-up value stream map

3.1.2 Resin Transfer Molding

The resin transfer molding process also starts at the weaving company, with the same waste sources as outlined above (Figure 23). Unlike hand lay-up, resin transfer molding does not involve prepregging. Instead, the dry fabric is laid directly into a closed mold and resin is injected (transferred) to form a part. Instead of prepreg scraps from ply cutting, there are fabric scraps, which possess less material value. This process, like most composite forming processes, still has trimming waste, though there is less waste than in hand lay-up, as resin transfer molding is able to form near-net shape parts. Another advantage of resin transfer molding is that it is an out-of-autoclave process, which equates to lower cycle times and cost.

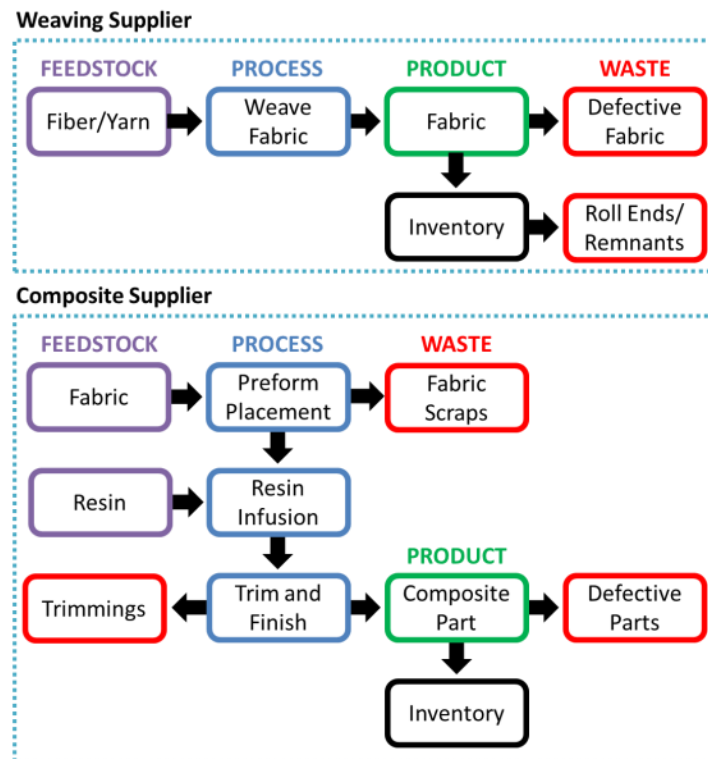


Figure 23: Resin transfer molding value stream map

3.1.3 Automated Tape Placement

Figure 24 shows the value stream map for automated tape placement. Unlike hand lay-up and resin transfer molding, automated tape placement uses unidirectional tapes instead of fabrics. As a result, there is no weaving step and fiber is provided directly to the prepreg manufacturer. The prepreg manufacturer will make wide tapes (several inches at least) from multiple filament yarns. These tapes are then slit to the width specified by the customer. In addition to waste caused by expired material, some material is also lost during the slitting process, particularly at the edges of the tape. At the composite manufacturer, a tape placement machine is used to lay down the prepreg tapes, directly from spools. The advantage of automated tape placement is that it automates the lay-up process, increasing productivity and eliminating waste from cutting plies. Trim is still necessary to attain the final shape of the composite, which results in trimmings waste. Automated tape placement is probably the leanest composite manufacturing process used today; unfortunately, it is very limited in the types of composites that can be produced. Automated tape placement is only able to lay unidirectional tapes and due to the large size of the lay down head, it is restricted to parts with minimal contour.

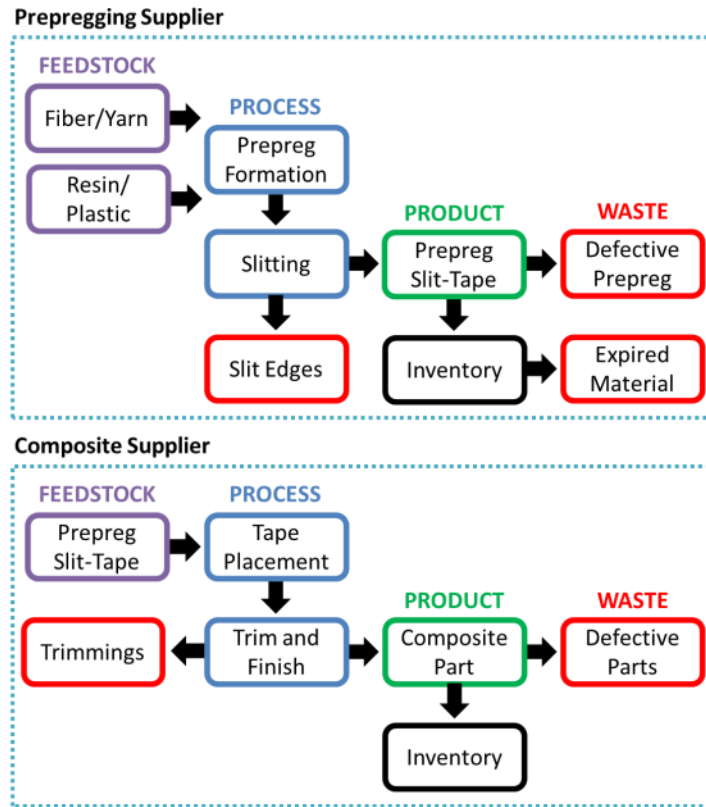


Figure 24: Automated tape placement value stream map

3.1.4 Compression Molding

As described in the literature review, compression molding processes are generally not used for high-performance composites; however, the evolution of compression molding from sheet molding compound (SMC) to direct long fiber thermoplastic molding (DLFT) can be used as a template for lean optimization of a manufacturing value stream. Figure 25 shows the value stream map for compression molding with sheet molding compound, while Figure 26 shows the value stream map for direct long fiber thermoplastic molding. By chopping the fiber and compounding the fiber-polymer mixture at the composite manufacturer, it is possible to completely reduce the value chain to a single company. This reduces the opportunity for waste and allows the composite

manufacturer greater control over the properties of the final part, as they can adjust fiber-polymer ratios and material combination in response to customer demand. Previously, a composite supplier would have had to maintain an inventory of various types of sheet molding compound, and even then, may not have had the right product in stock when a customer order arrived.

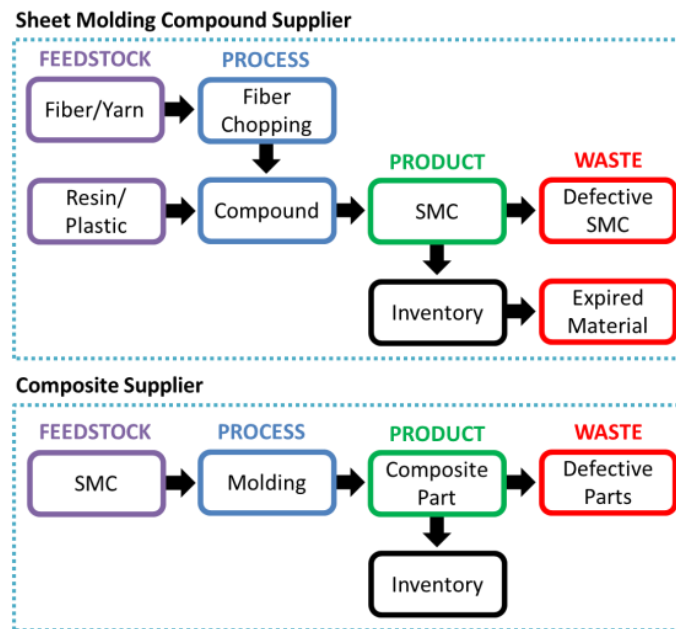


Figure 25: Compression molding (SMC) value stream map

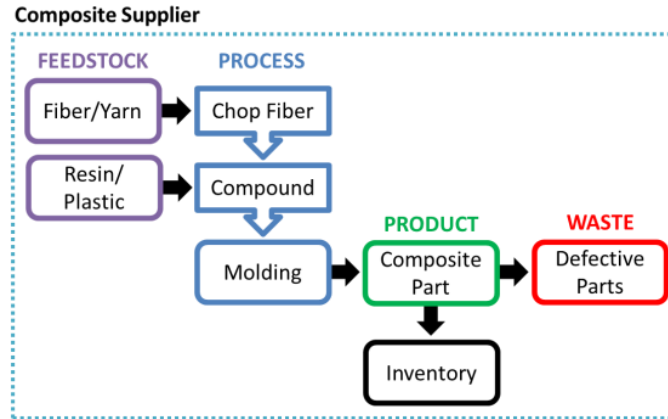


Figure 26: Compression molding (DLFT) value stream map. In this process, chopping and compounding occur simultaneously and feed into the molding step.

3.1.5 Generalization of Ideal Composite Forming Process

Based on the compression molding example, it is possible to generalize a composite manufacturing process that decreases value stream waste and increases productivity. In an ideal composite manufacturing process, the number of suppliers would be minimized and the composite manufacturer would have control over material properties. Furthermore, waste materials should be captured and reutilized in the manufacturing process. In this thesis, we are specifically interested in forming woven, thermoplastic composites. Woven composites require continuous fibers, which leads us to selecting prepreg tapes as a feedstock material for the composite manufacturing process. This necessitates a prepregging process; however, thermoplastic tapes are generally shelf stable and slit edges can be captured and reprocessed along with other waste generated at the composite manufacturer. This allows prepreg tape to be a viable option for a lean composite manufacturing process.

While material waste is one type of waste that lean manufacturing seeks to reduce, it is also focused on streamlining inefficient production caused by poor capital utilization or waiting between process steps. Production methods can be classified as job, batch, or flow production. Job production is best suited to producing one-off or made-to-order products. Batch production is suitable for low-volume manufacturing, while flow production is required to support high production volumes. Batching of parts through the batch production process results in machine downtime and inventory build-up between batches. Most composite manufacturing processes used today are batch processes that were developed for the aerospace industry, where low-to-medium volumes are expected. This makes scale-up expensive and has limited the adoption of composites in other industries. An ideal composite manufacturing process should be designed to support medium-to-high volume, which necessitates continuous feedstock at the very least and preferably continuous product as well. Continuous production would maximize capital utilization and eliminate waiting between process steps. Figure 27 illustrates an ideal value stream map for forming thermoplastic woven composites. This value stream includes the prepreg process, the composite manufacturing process, and the waste reuse processes. For the purpose of idealization, it can be assumed that composite manufacturing occurs over an arbitrary number of process steps (ranging from 1 to N), which convert the prepreg tape into a woven composite with complex contours.

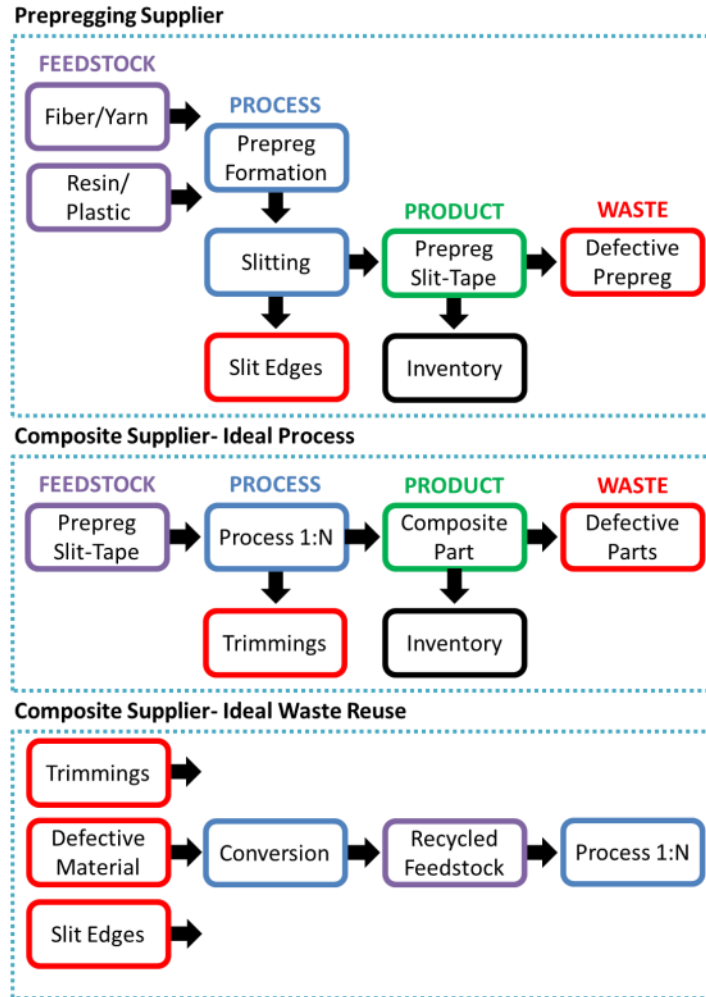


Figure 27: Ideal composite manufacturing process value stream map. Waste produced during the manufacturing process can be recycled and integrated into the composite during one of the processing steps

3.2 Design Theory

Design theory describes how a designer chooses to approach a particular problem. In this work, process analysis is used to analyze existing composite manufacturing technologies and uncover elementary steps. After process analysis, it is necessary to apply design axioms to determine functional requirements. The functional requirements are based on the problem definition, which varies depending on who is defined as the

customer. By combining functional needs, lean manufacturing principles, and elementary steps, it is possible to synthesize a novel composite manufacturing process. This approach can be generalized to many other manufacturing approaches that currently rely on batch processing.

3.2.1 Elementary Steps of Composite Manufacturing

To develop a composite manufacturing process that meets the lean manufacturing requirements, it is first necessary to decompose the concept of composite manufacturing into elementary steps. This approach to invention and innovation is described Tadmor's "Machine Invention, Innovation, and Elementary Steps." [43] Tadmor explains that the process of converting polymer pellets into a finished product can be described by five elementary steps and five shaping steps. A similar approach can be applied to weaving and composite manufacturing. Weaving can be defined by three elementary steps: warping, shedding, and filling [15]. Warping is the process of aligning a number of yarns in parallel to create a warp. Shedding is the process of separating the warp yarns to two layers, which forms an opening called a shed. Filling, also known as weft insertion, is the process of passing the weft yarn through the shed. When the shedding process repeats, the weft filament is locked into position. For thermoplastic composite manufacturing, it is necessary to define both elementary and shaping steps (Table 2). Given that thermoplastics are most commonly formed into prepregs prior to forming the part, one or more elementary steps may be repeated.

Table 2: Elementary Steps and Shaping Steps for Composite Manufacturing

Elementary Steps	Shaping Steps
Fiber/Fabric Placement	Molding
Infiltration	Calendering
Melting	
Consolidation	

An example process that uses these elementary steps is as follows: During the prepregging process, the thermoplastic polymer undergoes *melting* before it is *infiltrated* into the fibers/fabric. This combination of materials is *calendered* (a shaping step) to remove excess polymer and create a prepreg tape/fabric. During composite part *molding*, the prepreg tape/fabric is *placed* in the mold before the polymer is *remelted*. While the polymer is still in the molten state, pressure (and sometimes vacuum) is applied to *consolidate* the composite, removing air from the composite and bonding the various layers together.

These elementary steps represent the lowest common denominator of existing composite forming processes; however, each process approaches these steps in a different fashion. Regarding the elementary step of consolidation, hand lay-up traditionally achieves consolidation through the application of vacuum pressure or autoclave pressure, while automated tape laying and compression molding rely on mechanical pressure. In the case of automated tape laying, this pressure is applied by a roller. In compression

molding this pressure is achieved by squeezing the composite between matched molds. In resin transfer molding, there is a combination of mechanical pressure from the molds and fluid pressure from the resin that is injected into the mold cavity. Similarly, melting of the thermoplastic composite can be achieved through either direct heating (radio frequency, microwave, induction) or indirect heating (convection, conduction, infrared radiation) of the composite. In the former case, the composite is heated uniformly; while in the latter case, the heat is generated at the surface of the composite and then must be conducted throughout the thickness. The majority of existing composite forming processes utilize indirect heating methods; however, direct heating has become a promising area of study as researchers seek to reduce cycle time and processing cost. For the production of thermoplastic prepregs, the elementary step of infiltration is achieved by passing dry tows through a bath of molten plastic. Alternate methods of infiltration include combining thermoplastic fibers with reinforcement fibers in blended tows and spray coating or extrusion coating of dry yarns with thermoplastic resin. In these alternate cases, final infiltration is not achieved until additional heat and pressure is applied to force the resin to wet-out the fibers. This can be achieved as part of the filament production process, or it can occur during final consolidation of the composite. Finally, placement of fibers/fabrics can be accomplished by a laying process (such as hand lay-up or automated tape laying) or through the use of preforms (commonly used in resin transfer molding).

These examples show that the elementary steps are intended to be categorical, rather than descriptive. As technology develops, new methods of achieving a specific

elementary step may be conceived which in turn may result in the development of new composite forming processes.

3.2.2 Design Axioms

An axiomatic approach to design was proposed by Nam Suh in “The Principles of Design” [44]. The text defines only two axioms, but additional corollaries and theorems can be derived from these axioms and utilized as guidelines during the design process. The first axiom states “maintain the independence of functional requirements” [44]. For a design that combines multiple functionalities, as most designs do, this means that changing design parameters for one function should not affect the other functions. The second axiom states “minimize the information content” [44]. Information content is broadly defined as everything from the design drawings of individual parts to the time required to machine each component. Broadly interpreted, the information axiom advises the designer to seek simple solutions and encourages interchangeable parts with high tolerance.

3.2.3 Functional Requirements, Constraints, and Design Parameters

Functional requirements (FRs) are determined by customer needs. For this work, we will consider two customers that currently use composites: the aerospace industry and the automotive industry. Both of these customers use composites to reduce vehicle weight; however, they have very different needs when it comes to production volume, price tolerance, and desired mechanical properties. Composite manufacturing methods are widely used in the aerospace industry because they are able to meet the volume and price

targets. Composite use is much more limited in the automotive industry as current methods do not meet volume and cost targets for mass production.

The aerospace industry is seeking innovations that offer better weight reduction than existing composites, while still utilizing current molds and materials. This allows us to define the global FRs and Constraints as:

FR1: Reduce mass while maintaining or improving strength and stiffness;

C1: Maintain compatibility with conventional tooling for wing/fuselage panels;

C2: Utilize existing FAA-approved feedstock materials.

In the automotive industry, the objective is to replace metal parts with composite parts to reduce vehicle weight. They are also interested in reducing part numbers through part integration. The industry must also meet rate demands, regardless of weight savings. The global FRs and Constraints can be written as:

FR1: Reduce the cost of manufacturing a composite part to within 10% of a metal stamped part;

FR2: Reduce the number of parts through part integration;

C1: Minimum annual production rate of 250,000 parts.

Once the global FRs and Constraints have been determined, it is necessary to conceptualize a physical design that can fulfil the FRs and Constraints. Once a physical concept has been conceived, the designer can determine the functional requirements for that concept and iteratively alternate between the functional space and the physical space

to develop a hierarchy of functional and physical requirements. Design parameters (DPs) are used to link the functional space to the physical space. DPs have the potential to become constraints at lower levels of the hierarchy, so it is important to consider the potential implications when deciding on the physical design. DPs should be selected such that independence of the FRs is maintained. If changing a single design parameter would affect more than one functional requirement, it means that the functional requirements are not truly independent, and it may be necessary to redefine the FRs or DPs.

3.3 Synthesis

Based on a review of the literature and evaluation of existing composite manufacturing processes, there is a need for an automated method of composite forming that can create woven composite structures. Several of the previously described concepts can be combined to create a method that may be used to design lean manufacturing processes.

The hierarchical approach to design is generally presented as a top-down approach, starting with the definition of global FRs and working down to the level of individual parts; however, by considering the elementary steps of composite formation and weaving, one can simultaneously approach the problem from both top-down and bottom-up. Referencing the global FRs and constraints for the automotive and aerospace industries, additional global FRs can be applied to represent the lean manufacturing approach to process development:

FR1: Material waste should be minimized or reused within the manufacturing process

FR2: Inventory steps should be minimized

FR3: Flow production should be maximized

Based on the prior assessment of composite manufacturing processes, an ideal manufacturing process was proposed that utilizes the same slit tape feedstock that is found in thermoplastic automated tape placement. This provides a starting point for defining the process steps needed to produce woven, thermoplastic composite structures. By applying the elementary steps to the feedstock, any proposed composite forming machine will need to include warping of the slit tapes, shedding, weft insertion of slit tapes, slit tape placement, melting of the slit tape, consolidation of the slit tape and at least one shaping step. The order of process steps can be determined by evaluating the design parameters of each elementary step and relating them to the FRs. Slit tape selection occurs during the warping step; therefore, the design parameters include fiber type, polymer type, tape dimensions, fiber volume fraction, and warp tape spacing. The shedding and weft insertion steps can be considered together when defining DPs, since one cannot occur without the other. The DPs for these two steps are weave pattern, weft spacing, and weaving rate. The DPs relating to slit tape placement are placement rate and placement angle, and the DP for the melting step is melting rate. Finally, consolidation has the design parameters of consolidation pressure and cooling rate. These DPs can be related back to the global FRs, allowing related hierarchies to be identified. Figure 28 shows the relationship between DPs, elementary steps, and the global FRs. Aerospace- and automotive-specific FRs are shown on the left side and are related to the design parameters, while the Lean FRs are shown on the right side and are connected to elementary process steps.

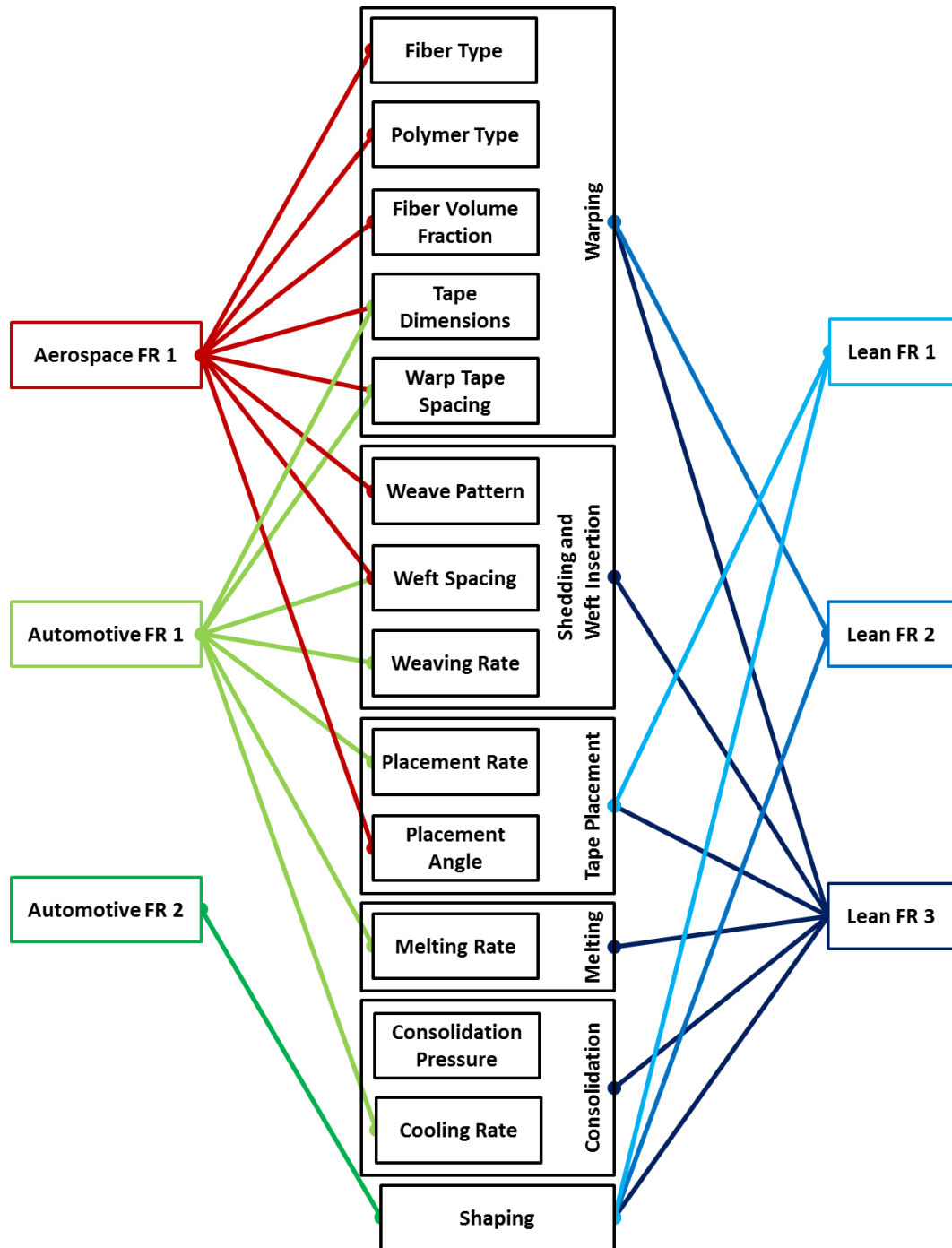


Figure 28: Mapping of Functional Requirements and Design Parameters. Market-specific functional requirements are on the left, lean functional requirements are on the right. Design parameters are shown in the middle and grouped by elementary steps. Colors are used to identify which design parameters are related to which FRs

Now that a relationship has been developed between the elementary steps and the global FRs, it becomes apparent that the design parameters between the automotive and aerospace FRs are largely unrelated. This leads to the conclusion that these industries require different solutions to meet their functional requirements. CHAPTER 4 presents a machine and manufacturing process to address the aerospace functional requirement, while CHAPTER 5 presents a machine and manufacturing process to address the automotive functional requirements. In both case studies, the lean functional requirements are integrated into the manufacturing process.

CHAPTER 4. LAYER-BY-LAYER MANUFACTURING OF WOVEN COMPOSITES: MAGIC

4.1 Concept

The MAGIC composite forming machine was developed to address the aerospace FRs and constraints. The key DPs for aerospace FR1 (Reduce mass while maintaining or improving strength and stiffness) were identified as filament properties (fiber type, polymer type, and dimensions), warp spacing, weft spacing, weave pattern, and placement angle. In order to meet Constraint 1 (Maintain compatibility with conventional tooling for wing/fuselage panels), the prototype must match current molding and consolidation techniques used with automated tape placement. Similarly, Constraint 2 (Utilize existing FAA-approved feedstock materials) can be satisfied by using prepreg tapes currently used by automated tape placement. MAGIC sought to address aerospace FR1 by blending additive manufacturing concepts with existing composite manufacturing technologies, such as automated fiber placement. Fused filament fabrication offers very precise control of head position and filament laydown path; however, it is generally limited to depositing a single filament at a time. On the other hand, automated fiber placement is able to lay down multiple filaments simultaneously, but the deposition head is not able to independently control the laydown path of each filament. Both of these technologies are also unable to form woven structures, which limits their impact resistance and their ability to tailor the properties of composite materials.

The solution that was developed involves independent control of multiple filament deposition heads that, when synchronized, enable the formation of woven structures. This allows the user to control weave density and weave patterns, even to the point of weaving multiple layers together to form a delamination-resistant structure. In the MAGIC machine, we designate filament deposition heads as either warp or weft print heads. Much like the warp beam in a weaving loom, the warp print heads are constrained to move parallel to one another in a single axis (termed a warp rack), while the (one or more) weft heads are able to move in two axes, one parallel to the warp heads and the other perpendicular to the weft heads. This allows the weft head to insert weft filaments between the warp filaments to create an interlacing pattern. A simplified depiction of this configuration for four warp heads and one weft head is shown in Figure 29. By adding additional warp racks and weft heads, it is possible to deposit multiple layers simultaneously and weave the layers together. This is achieved by allowing one or more warp heads from the second warp rack to move past one or more warp heads from the first warp head. A more complex diagram that shows all the steps for producing a plain weave can be seen in Figure 30.

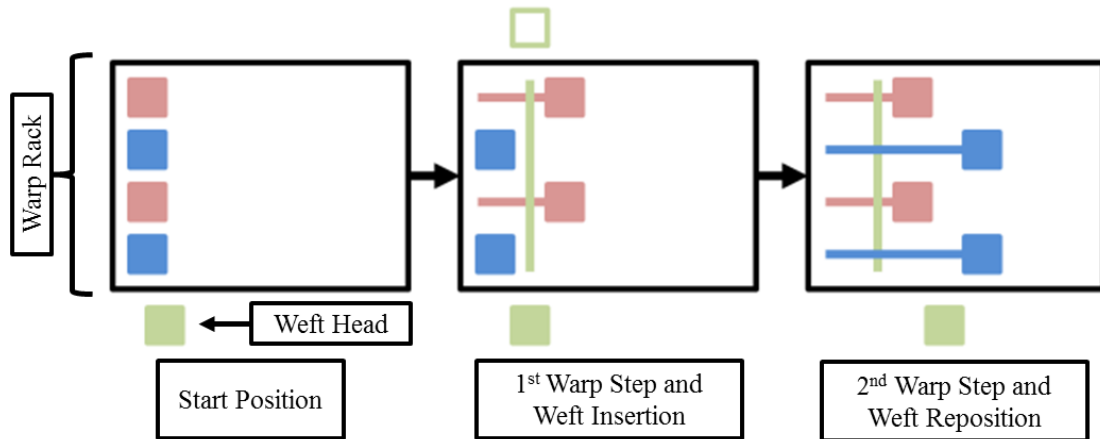


Figure 29: MAGIC interlacing method. Pink and blue boxes represent the first and second warp head groups, respectively. The green box indicates the weft inserter. Colored lines show filaments deposited from the respective heads.

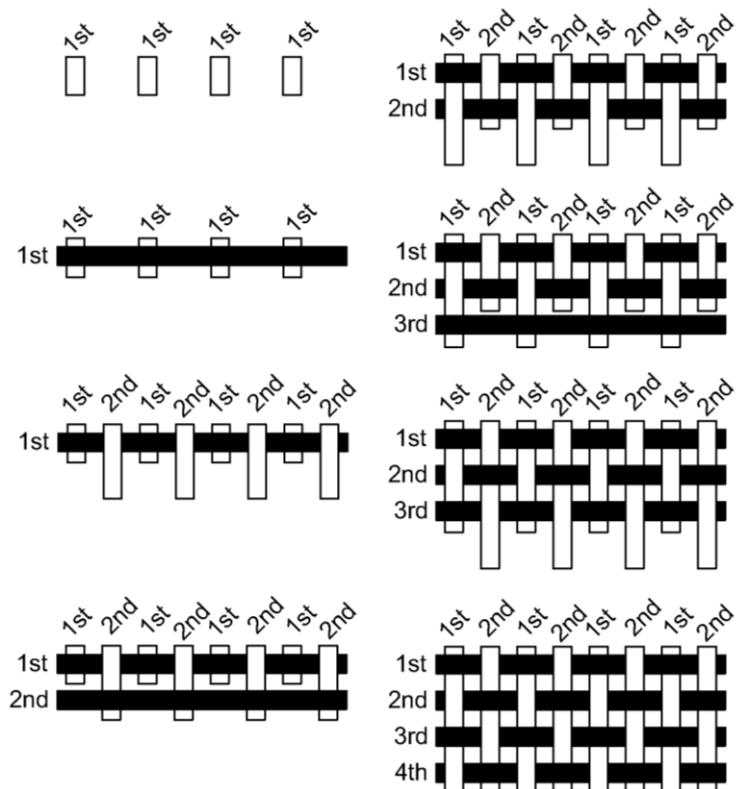


Figure 30: Method for forming plain weave structure. White boxes represent warp filaments, and belong to the 1st or 2nd warp group. Black boxes represent weft filaments. The deposition process starts at the upper left corner and proceeds down the left column, before continuing from the upper right column.

The ability to control individual warp yarns independently of one another offers many advantages. Each print head can be loaded with a different filament, allowing the creation of multi-material composite structures with properties that can vary across the composite. One subset of multi-material composites are functional composites, which may combine metallic filaments with insulating filaments (such as glass or Kevlar). In these structures, it would be possible to have a structural component that is also capable of carrying electrical signals (such as power or sensor data). Individual warp head control also allows the machine to operate as a 3D Jacquard loom, varying weave pattern within a single layer or between multiple layers; for example, from plain weave to satin weave (Figure 31). When combined with the ability to rotate the print bed to change warp alignment (relative to previously deposited layers), this allows composite designers to vary weave pattern, fiber material, fiber alignment and weave density to a degree not currently available in current composite manufacturing systems.

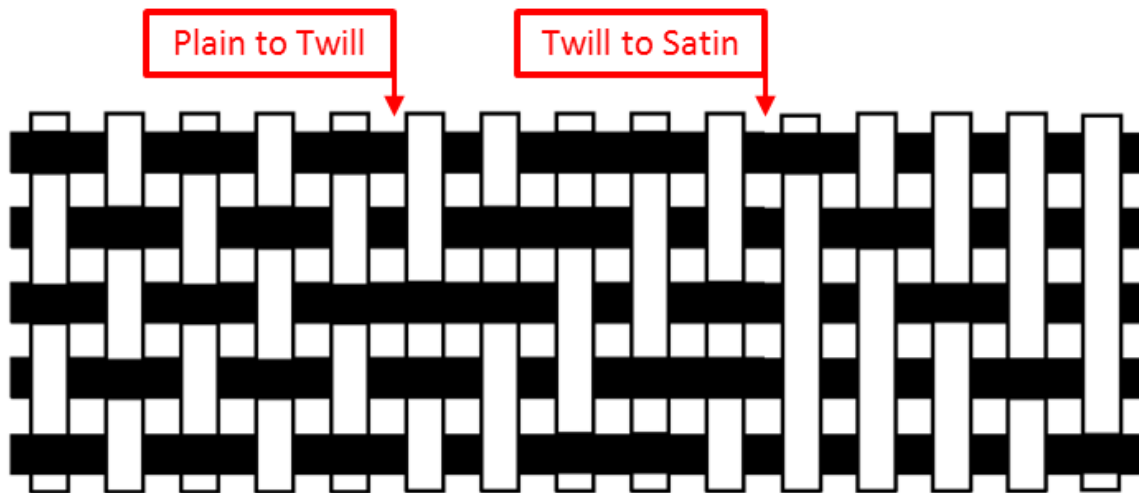


Figure 31: Weave transition, plain to twill to satin. Transition points are indicated.

4.2 Implementation

A mock-up of the MAGIC machine warp heads and roller was constructed in the fall of 2014 (Figure 32). This mock-up demonstrated that it was possible to weave both 2D and 3D fabric geometries using two warp racks. The mock-up relied on manually positioning the warp heads and manual insertion of the weft filament. Following the completion of the mock-up, a proof-of-concept model was constructed with four warp heads to demonstrate that head temperature could be controlled and to test the ability to position heads using a lead screw driven by a stepper motor. Weft insertion was still performed manually and the print surface was fixed, with neither vertical nor rotational motion. The proof of concept system was completed over the summer of 2015 (Figure 33).

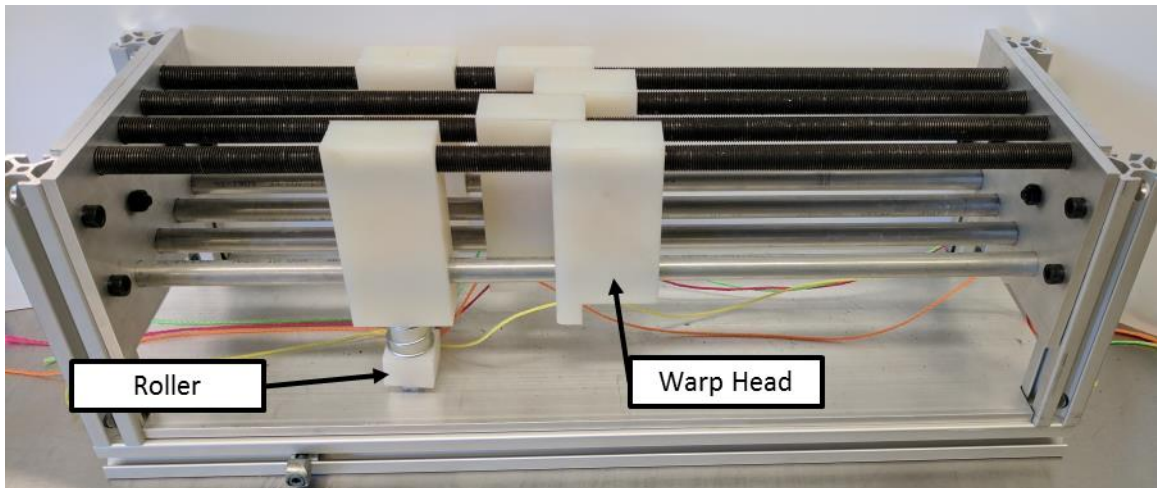


Figure 32: Mock-up of MAGIC machine warp heads and roller. Mock-up enabled validation of weaving capability by sliding the warp heads into various positions.

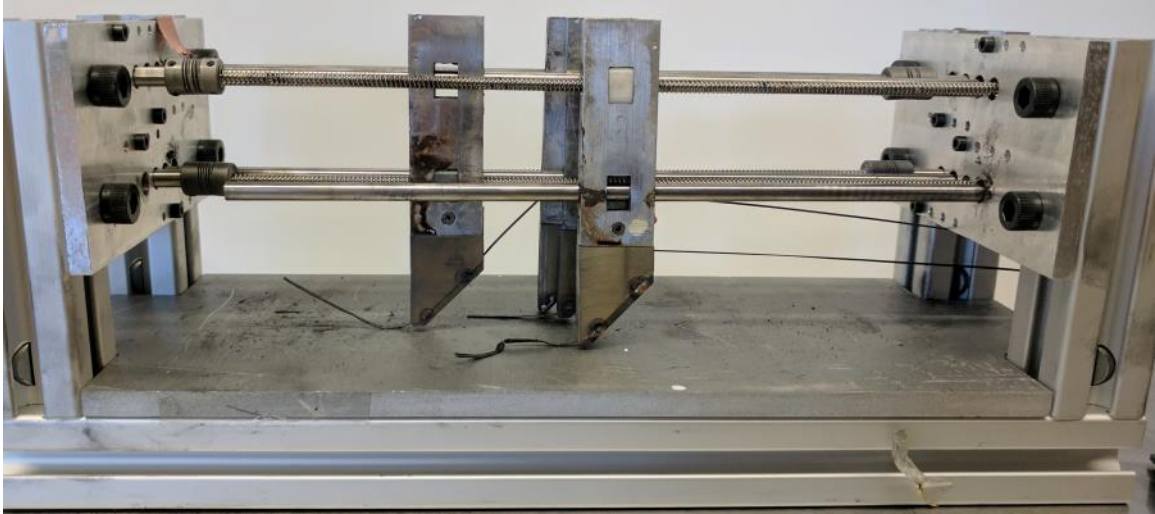


Figure 33: Proof-of-concept of MAGIC machine warp rack

Figure 34 shows a representation of a single warp head from the proof-of-concept machine. Each warp head is restricted to move along a single axis, guided by a linear shaft and driven by a lead screw. Within each print head are a heating element and a temperature sensor, which are used to heat the print head to the melt temperature of the thermoplastic resin. The composite filament enters the print head at room temperature and leaves at melt temperature. In the full design, a heated roller would move along behind the warp heads, compressing the deposited filament and bonding it to the layers below.

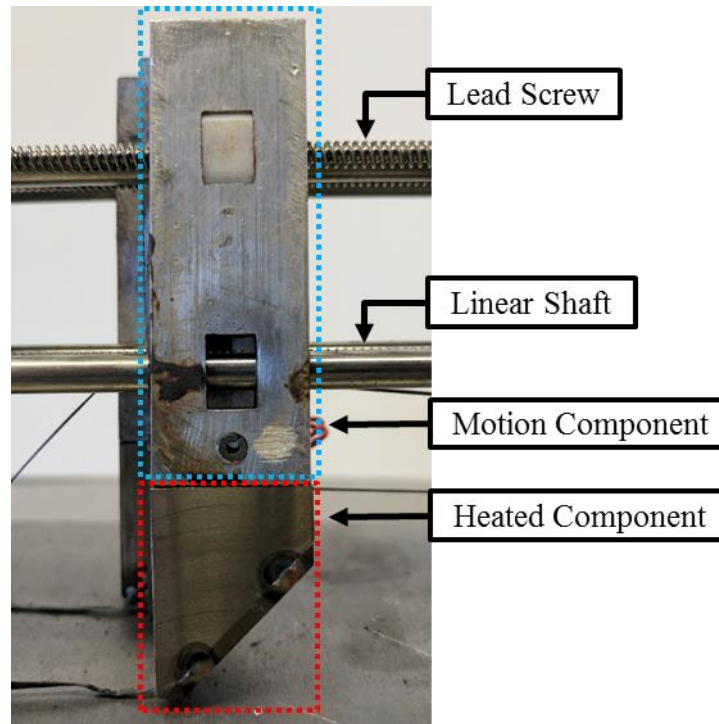


Figure 34: Proof-of-concept warp head. Note the discoloration around the linear shaft caused by lack of insulation between the heated and motion components.

One of the major lessons from this model was the importance of insulating the heated print head from the motion system. During one test of the heating system, the print head took more than 5 minutes to reach the equilibrium set temperature of 360°C. After running the system for 60 minutes, the molybdenum disulfide-silicone grease on the linear shafts was beginning to show evidence of discoloration and “cook-off”. This discoloration can be clearly seen in Figure 33 and Figure 34. After the print heads had returned to room temperature, further inspection revealed that the hardened steel linear shafts had warped slightly, likely a result of coefficient of thermal expansion (CTE) mismatch between the steel shaft and aluminum print head. Later versions of the warp print heads utilized a glass-mica ceramic insulator between the upper print head (motion system) and the lower print head (heater system) (Figure 35). This addition of the

insulator, combined with a smaller heated component, reduced the time to reach equilibrium temperature to less than 60 seconds and eliminated issues of heat transfer into the motion system.

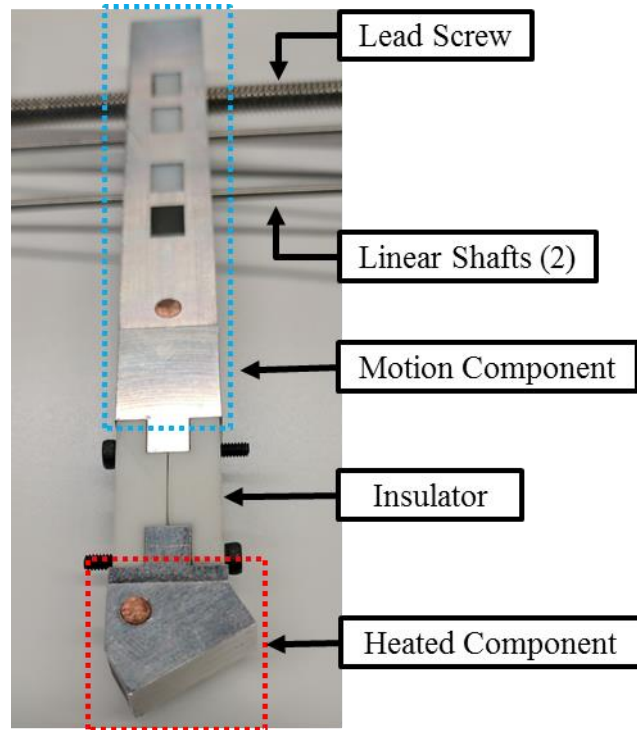


Figure 35: Bench-scale prototype warp head, side view. This view is presented to emphasize the addition of the insulator and the redesigned heated component.

At this point in the design development, weaving, temperature control, and warp head control had all been demonstrated separately and it was decided to proceed with scale-up to a 20-warp head prototype, with two racks of 10 heads each. This prototype would add weft insertion functionality and a print surface capable of vertical motion, while combining temperature control, warp head control and weaving into a single device. Construction of the prototype began in the fall of 2015, and by December we had assembled and tested the print plate subsystem, the weft inserter subsystem, and one full

rack of 10 print heads. Figure 36 shows the bench-scale prototype partially assembled to include both the warp rack and the print plate. The weft inserter is not shown.

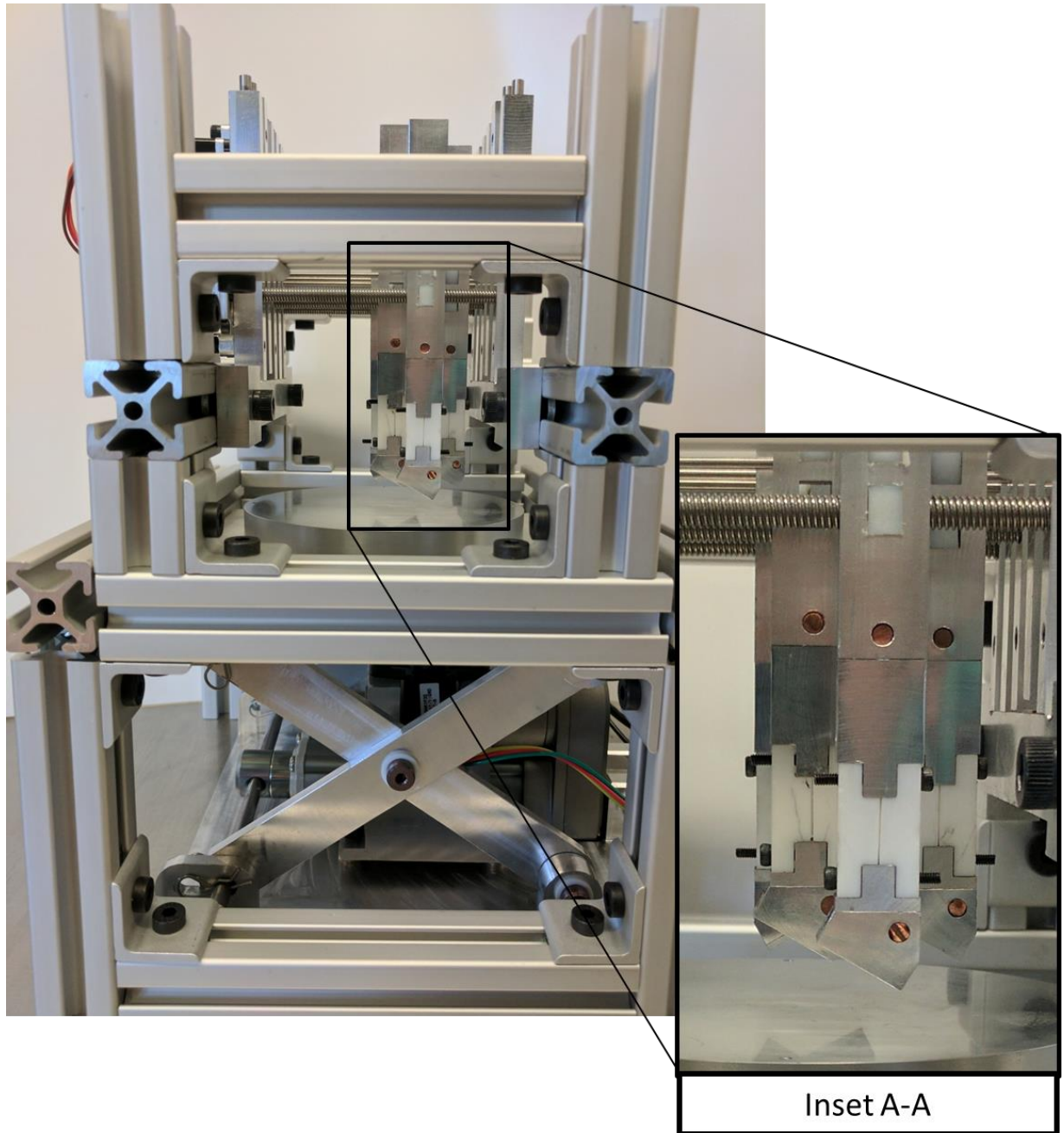


Figure 36: Bench-Scale prototype of MAGIC machine. This side view shows a single warp rack, print bed, and Z-stage. Inset A-A shows a close up view of the warp heads and the print bed.

4.3 Outcomes

During construction of the MAGIC prototype, a continuous composite forming machine design (WEAV3D) was conceived as a way to solve some of the issues discovered during prototyping of the MAGIC machine. Funding was secured from the Georgia Research Alliance to build a prototype of WEAV3D machine for the purpose of comparing this machine against the MAGIC prototype. After conducting some 100 customer discovery interviews over the summer of 2016, it was decided that WEAV3D had better immediate commercial potential and further development of MAGIC was suspended.

Many of the lessons from the design and construction of the MAGIC prototype were directly translated into the WEAV3D machine, even though the MAGIC prototype was not taken to completion. The importance of insulation between heaters and motion was transferred directly from MAGIC to WEAV3D. Furthermore, we were able to reuse many of the circuit boards designed to control the MAGIC machine with minimal changes, and some of the challenges with designing the roller and weft inserter for the MAGIC prototype led the team to solicit engineering assistance from the Georgia Tech Research Institute (GTRI) to design the rollers and weft inserter for the WEAV3D machine. This collaboration dramatically reduced the time required to produce the WEAV3D prototype.

4.4 Evaluation

Even though the subsystems of the MAGIC prototype were not fully integrated, it is still possible to evaluate the design in the context of the aerospace and lean functional

requirements. Since the MAGIC prototype is designed to utilize poly-ether-ketone-ketone (PEKK) and poly-ether-ether-ketone (PEEK) tapes already used for automated tape placement in the aerospace industry, the constraint of using FAA-approved feedstock was easily fulfilled. In order to comply with the molding constraint, the MAGIC prototype utilizes a roller-based laydown method that is similar to the one used for thermoplastic tape laying. To meet aerospace FR1 (reduce weight and maintain or increase strength and stiffness), the MAGIC prototype was designed to vary several design parameters during composite formation, including weave pattern, placement angle, and weft spacing. During machine set-up, the user can also set warp spacing and select the filament load-out for each print head. Figure 37 shows the physical hierarchy of the MAGIC prototype and relates the physical systems to the design parameters, FRs, and constraints.

While the global aerospace FR1 is influenced by a number of different physical systems, each system corresponds to a single design parameter, with the exception of warp and weft feedstock, which are both dependent on filament properties. This 1:1 relationship implies that the hierarchical FRs are independent, which satisfies Axiom 1 of Principles of Design [44]. Two additional physical systems, plate heating and head heating, are not directly linked to the global aerospace FR. This is because these two systems do not directly affect the mechanical properties of the composite, but they are still necessary for processing the thermoplastic tapes used.

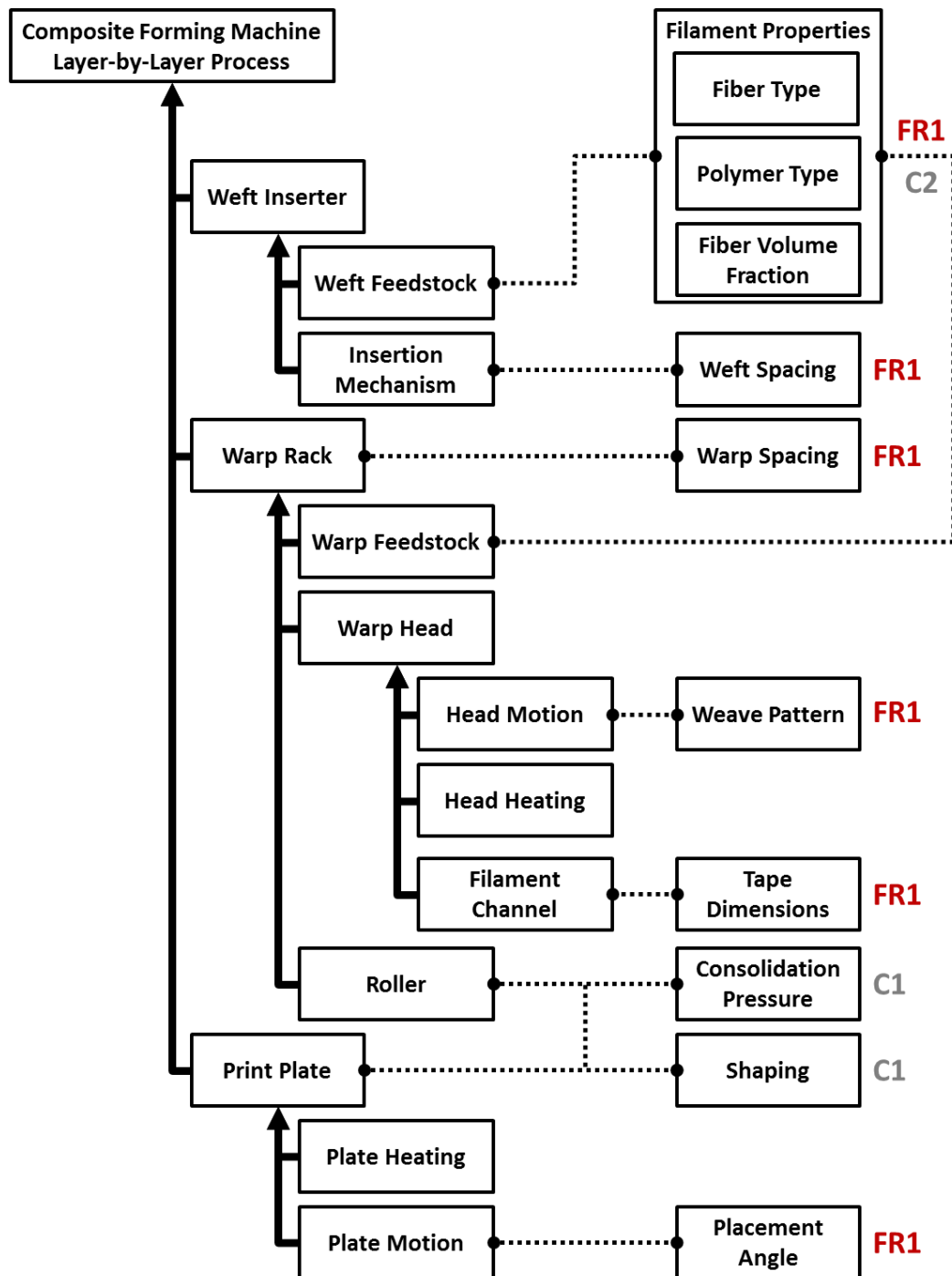


Figure 37: MAGIC physical hierarchy and design parameters. Aerospace FR1: Reduce mass while maintaining or improving strength and stiffness. Aerospace Constraint 1: Maintain compatibility with conventional tooling for wing/fuselage panels. Aerospace Constraint 2: Utilize existing FAA-approved feedstock materials.

Having satisfied the global aerospace FRs, it is necessary to evaluate the MAGIC prototype from the perspective of the global lean manufacturing FRs. From the perspective of lean FR1 (Material waste should be minimized or reused within the manufacturing process), the MAGIC system is material-efficient. Shelf-stable thermoplastic tapes are deposited individually and can be cut during deposition, meaning that very little material is wasted. Furthermore, the print bed is able to rotate between layers, allowing the formation of near-net-shape composites, which further reduces waste from trim operations. The MAGIC prototype also satisfies lean FR2 (Inventory steps should be minimized), which seeks to reduce inventory steps. Because weaving occurs during composite formation, we eliminate the fabric supplier from the value stream. This also reduces total inventory, because the composite manufacturer only needs to stock a selection of prepreg tape materials instead of maintaining a stock that includes multiple fabrics of multiple prepreg materials. The one area where the MAGIC design is inefficient is when it comes to flow production (lean FR3). The MAGIC prototype uses a continuous feedstock source but composite formation is still a batch process, and each piece must be removed from the mold before the next part can be formed.

In summary, analysis of the MAGIC prototype shows that it is capable of fully satisfying all of the aerospace and lean FRs, except lean FR3, which is only partially satisfied.

CHAPTER 5. CONTINUOUS COMPOSITE FORMING

MACHINE: WEAV3D

5.1 Concept

WEAV3D evolved from a desire to overcome several limitations inherent to the MAGIC machine. In particular, the layer-by-layer approach used by the MAGIC machine severely limits the build space and manufacturing speed. In order to overcome these limitations, it was necessary to completely discard some of the key features of the MAGIC machine, to attain the speed and build area required to meet the automotive FRs. The DPs that were identified for the automotive industry are tape dimensions, warp spacing, weft spacing, weaving rate, melting rate, and cooling rate. In addition, the MAGIC prototype did not fully satisfy lean FR3, which requires flow production. The ideal flow production system would utilize continuous feedstock and produce continuous product.

The first major change was to replace the print plate and roller with a system of paired rollers. This enables the production of composite sheets with fixed width, but arbitrary length. The second major change was to combine multiple warp filaments into a single warp head. This allows multiple layers of the composite to be fabricated simultaneously, but eliminates the ability to change the angle of the warp filaments between layers. Figure 38 shows a conceptual illustration of the WEAV3D machine. In this illustration, each warp head is threaded with four warp filaments and the warp rack consists of four warp heads. Warp filaments enter the heated enclosure at room

temperature. As they pass through the warp heads, the filaments are heated above the T_g of the polymer. The hot roller then heats the filament to the polymer's melt temperature and applies consolidation pressure. The temperature of the warp heads and hot roller can be adjusted in order to process different types of filaments. The insertion of the weft filaments occurs between the warp rack and the hot roller. After leaving the heated enclosure, the filaments pass through a number of progressively cooler rollers until they return to room temperature.

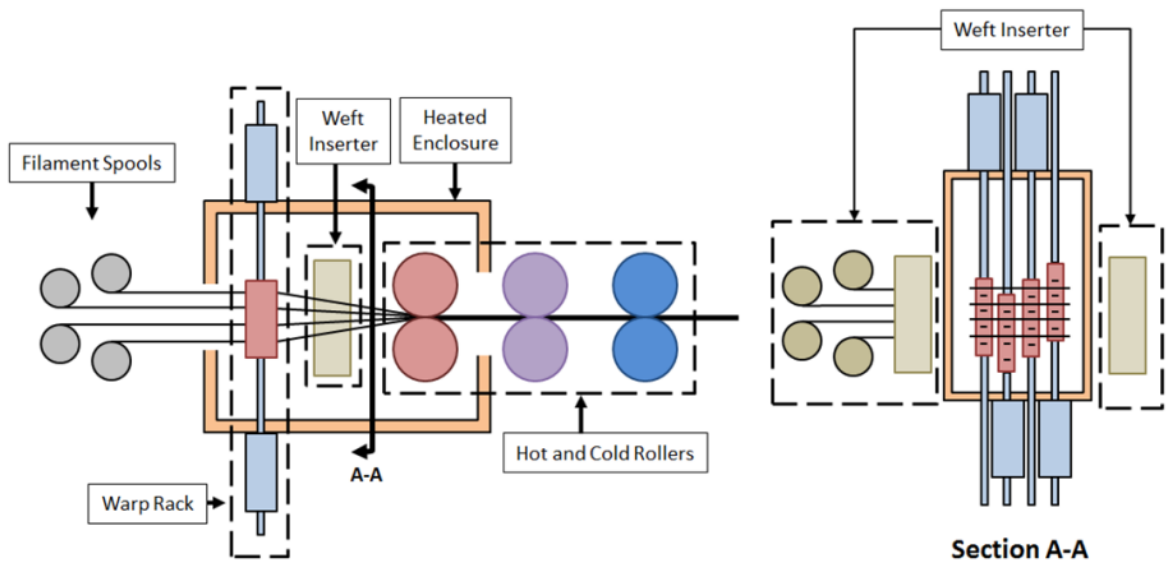


Figure 38: Diagram of WEAV3D machine. Left panel shows the side view of the machine. Filament spools shown in the left panel are warp filaments. Right panel is a cutaway along Section A-A, showing the warp rack and weft inserter in detail. Filament spools shown in the right panel are weft filaments.

5.2 Implementation

WEAV3D was conceived in November of 2015 and a mock-up was constructed in December of 2015 (Figure 39). This mock-up successfully demonstrated that combining multiple warp filaments into a single warp head would still enable the formation of both

2D and 3D woven structures. As a result, we decided to proceed with construction of a bench-scale prototype.

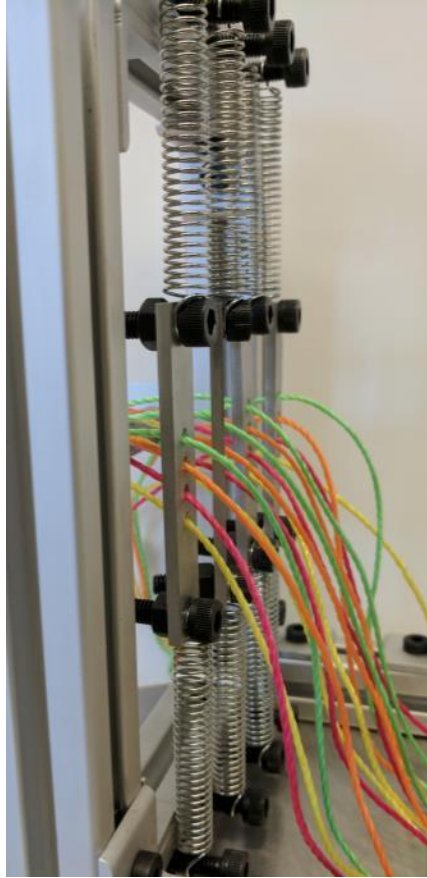


Figure 39: Mock-up of WEAV3D warp rack. Springs allow manual manipulation to explore the spatial relationship between the warp heads.

In order to generate samples of sufficient size for mechanical testing, we designed a warp rack consisting of 10 warp heads, each with four warp filament channels (Figure 40). This will allow for the production of samples that are 10 cm wide and four layers thick (approximately 1.5-2 mm, depending on filament thickness). Figure 41 shows a single warp head in profile, colored to show the temperature of components during operation. The middle of the print head contains the heaters and filament channels. Each filament channel is bracketed by a cartridge heater to heat the filament quickly and

uniformly, while the top and bottom of the heated portion contain temperature sensors to measure the equilibrium temperature. During composite formation, the warp heads are designed to heat the filament to a temperature between T_g and T_m of the polymer used in the filament. This reduces the amount of energy required for composite consolidation at the roller assembly. The heated component (which contains the filament channels) is designed to be replaceable to allow filament channels with different dimensions to be swapped in and out.

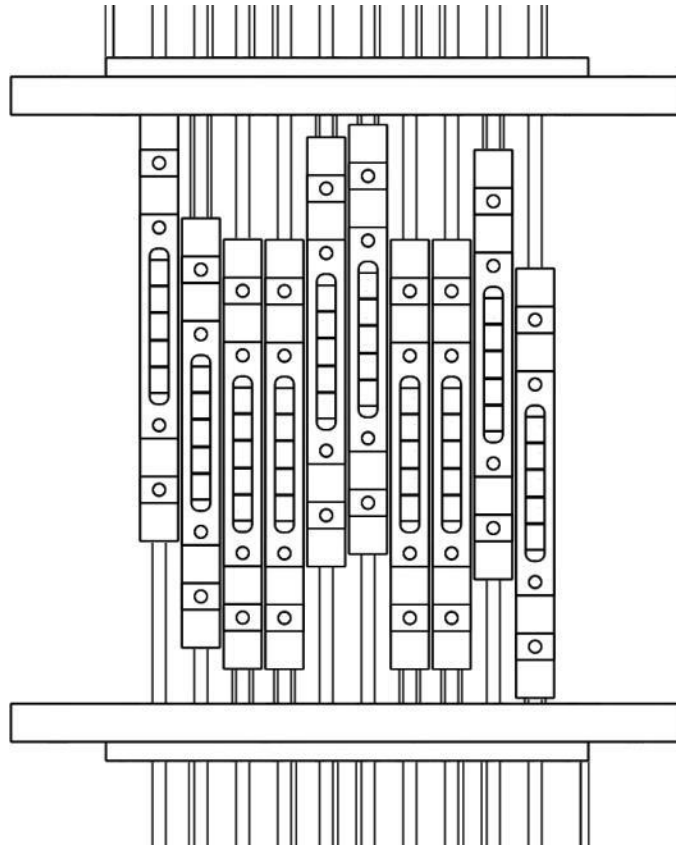


Figure 40: Front view of warp rack containing 10 warp heads. Warp filaments come out of the page.

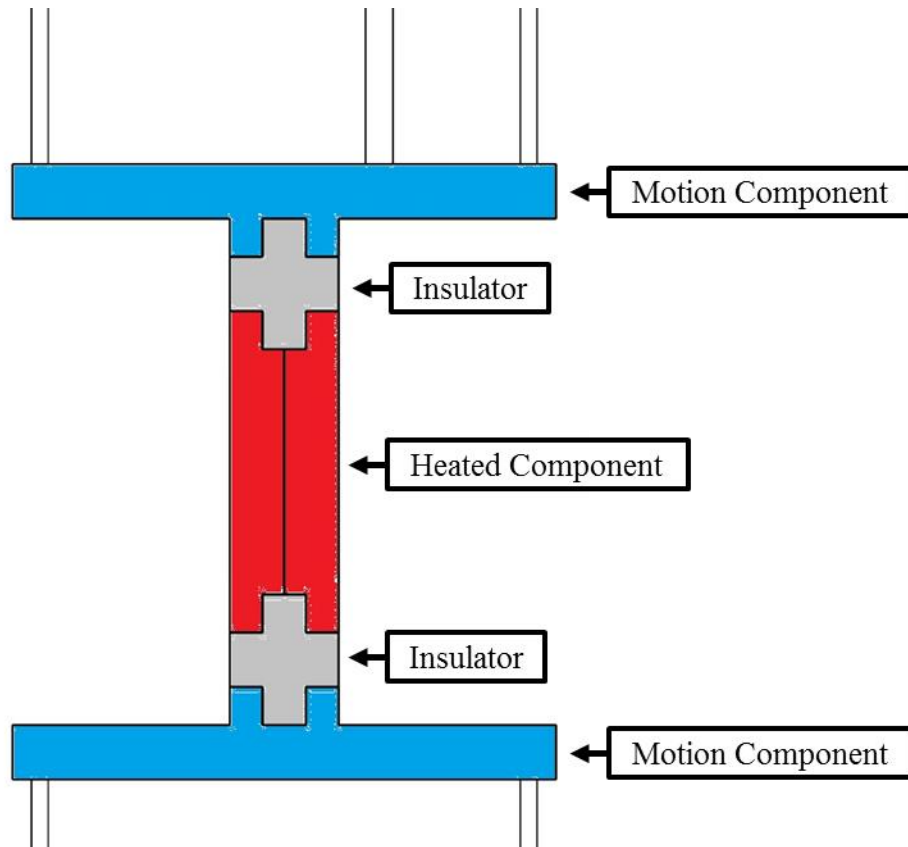


Figure 41: Side view of a single warp head, color-coded.

The top and bottom of the heated component are thermally isolated from the motion components by a glass-mica insulator. The motion component of the warp head utilizes a single lead screw and four linear shafts. While the MAGIC machine utilizes lead screws with an external lead nut, the WEAV3D machine uses non-captive internal lead nuts. The non-captive lead nut allows the lead screw to extend and retract without rotating; however, this applies torque on the warp head. The four linear shafts resist this torque and also stabilize the linear up-and-down motion of the warp heads during the weaving process.

The next key subsystem in the development of the WEAV3D machine was the roller assembly. The purpose of the roller assembly is to first consolidate the composite with

heat and pressure, before cooling it below T_g of the polymer. While the simplest implementation of the roller assembly consists of one heated roller pair and one chilled roller pair, more complex assemblies can have multiple heated rollers, each set to an incrementally lower temperature. This approach enables control over the crystallinity of the polymer. Figure 42 shows a CAD model of a roller assembly that contains one pair of heated rollers and one pair of cooled rollers. The outer casing has been made transparent in the model to make the internal components visible. The heated and cooled rollers are functionally identical, with the exception that the heated rollers have a cartridge heater installed, while the cooled rollers utilize a water-filled heat exchanger to remove heat from the system. Both pairs of rollers are driven by a chain and gear arrangement, which allows us to change gear ratio as needed. This system is used to “pull” composite filaments through the warp rack and into the rollers for consolidation. While each pair of rollers can be driven by a separate motor, we elected to use a single motor for the bench-scale prototype to reduce complexity. Finally, each pair of rollers relies on two pneumatic cylinders to apply pressure on the composite during consolidation and cooling. Two arms connect the rollers to the pneumatic cylinder, pivoting on the gear shaft and acting as a lever to transfer force from the cylinders to the rollers.

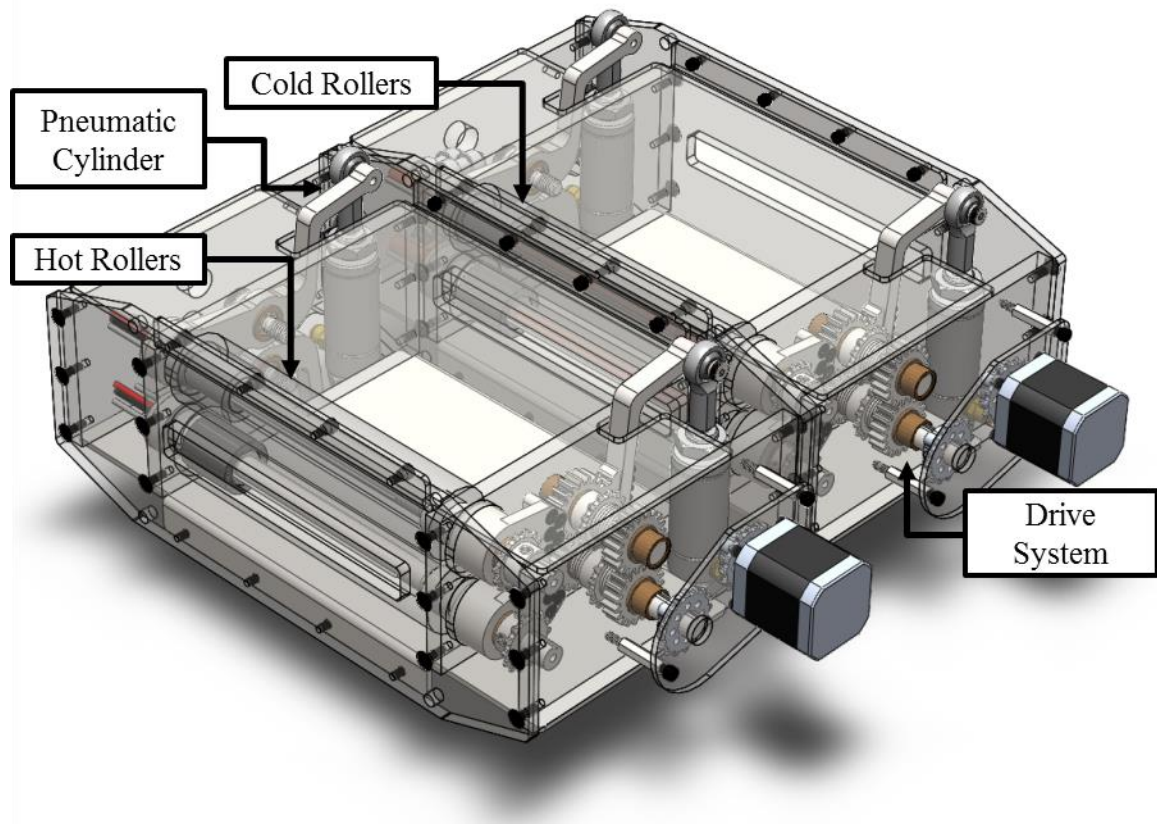


Figure 42: CAD model of roller assembly

The final subsystem required to demonstrate the function of the WEAV3D machine is the weft inserter (Figure 43). The WEAV3D weft inserter has several features that differentiate it from a weft inserter used in traditional weaving looms. The WEAV3D loom is designed to insert a rigid or semi-rigid resin-impregnated filament, unlike the flexible yarns used in traditional looms. This means that the filament does not require support during insertion, unlike traditional weaving looms which require support in the form of a rapier or air jet. As such, we can utilize a modified version of an inertial inserter. In this type of weft inserter, a roller is used to accelerate the filament across the width of the warp rack, before the weft filament is cut and “beat-up” into the rollers. Another benefit of the WEAV3D weft inserter is its ability to insert multiple weft

filaments simultaneously. This allows for all layers of the composite to be formed with a single weft insertion, dramatically increasing production speed. In order to control the spacing of the weft filaments as they leave the inserter, a guide plate is utilized. One advantage of this approach is the ability to swap out the plates as needed to change the spacing or add/remove weft filaments.

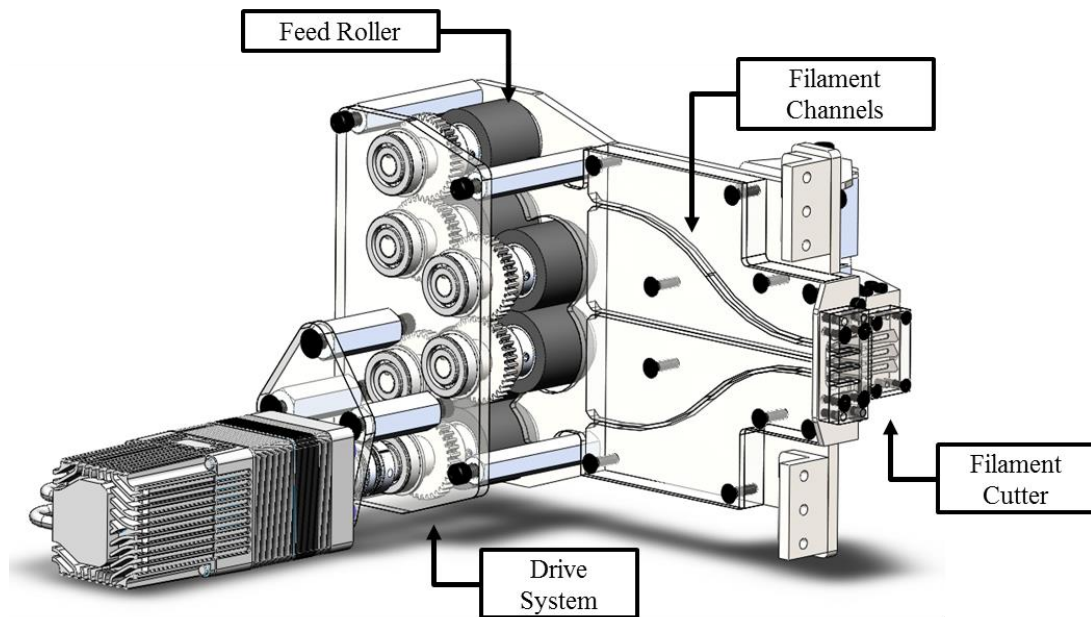


Figure 43: CAD model of weft inserter

Efforts were made throughout the design process to ensure that the WEAV3D machine would be scalable. Spacing of the warp heads and number of warp heads per rack can be changed by adjusting the spacing and number of holes in the warp rack mounting plate. Similarly the rollers can be widened by simply installing a longer roller and longer heater/heat exchanger. The weft inserter is designed to run all rollers from a single motor, through a gear stack, so additional weft filaments can be added by

increasing the number of rollers in the gear stack and increasing the number of filament channels in the guide plate.

5.3 Outcomes

A successful demonstration of the WEAV3D machine was conducted on June 21, 2017. This test integrated all of the individual subassemblies, using a step-wise control system to cycle through each step of the composite manufacturing process. During this test, a 1/1 plain weave was generated to demonstrate the ability to control warp head positions, insert weft filaments and consolidate the composite through the roller assembly. Figure 44 shows the WEAV3D machine after initial warping. Figure 45 shows the shedding step, prior to weft insertion. Figure 46 shows the composite lattice after passing through the hot roller. Finally, Figure 47 shows the composite lattice after it has exited the WEAV3D machine. This test utilized filaments with a width of 6 mm. Warp filaments were spaced 10 mm from center to center, while weft filaments were approximately 20 mm from center to center.

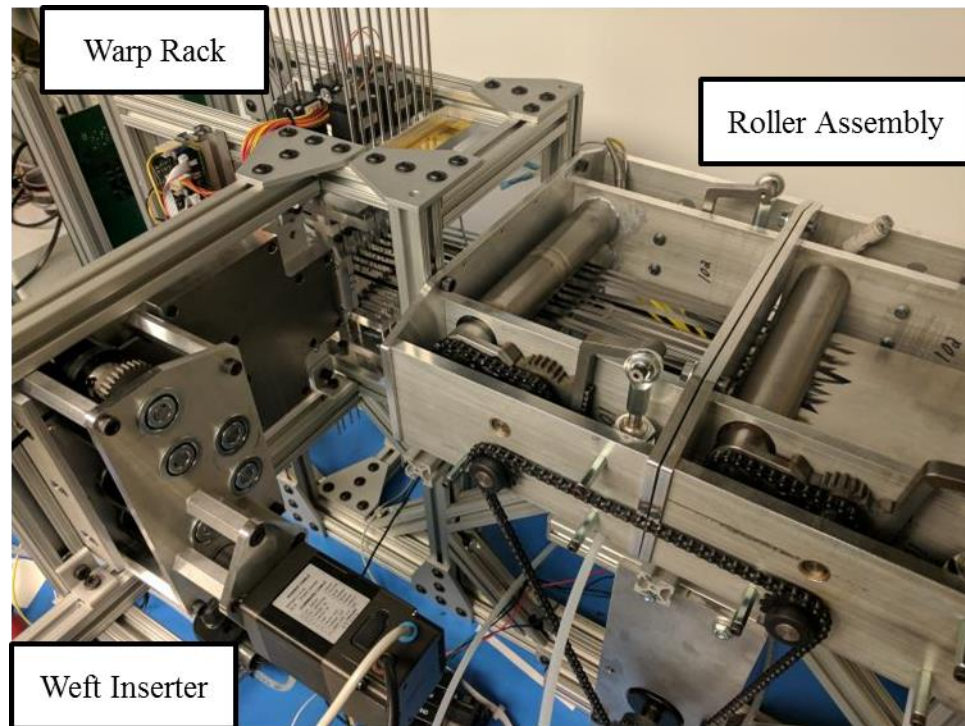


Figure 44: WEAV3D machine, after warping

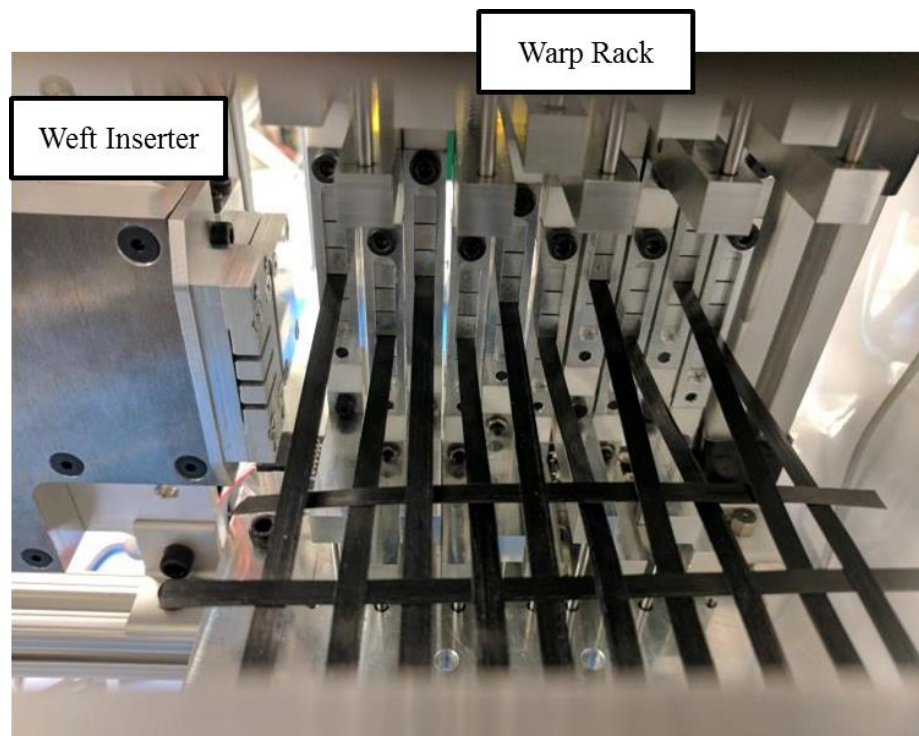


Figure 45: Close-up of WEAV3D shedding process.

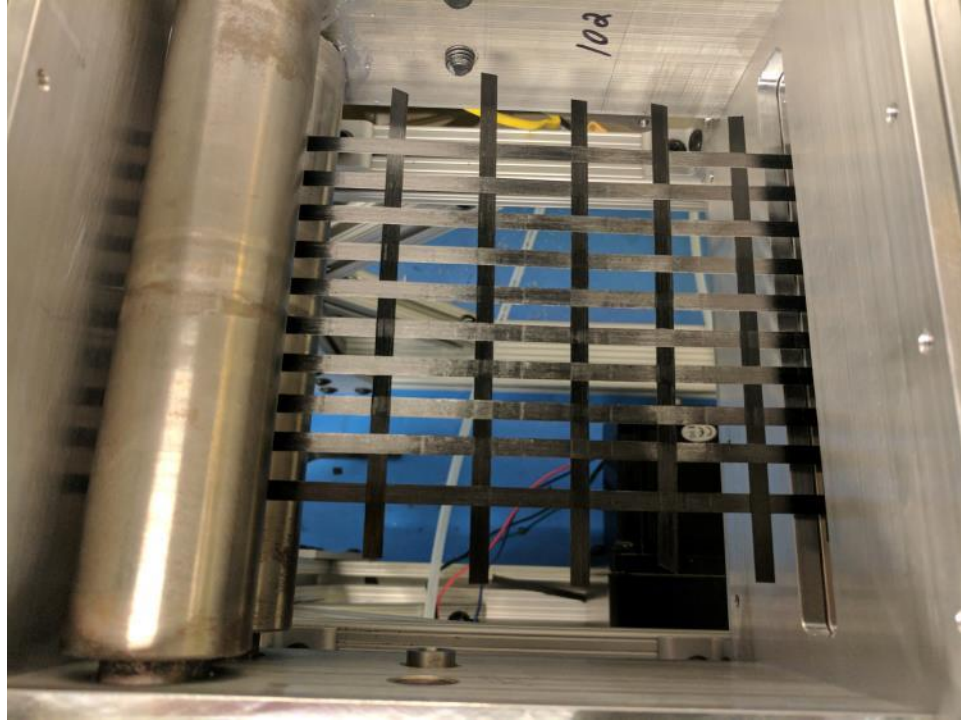


Figure 46: Composite lattice, exiting hot roller. Machine feed direction is from left to right.

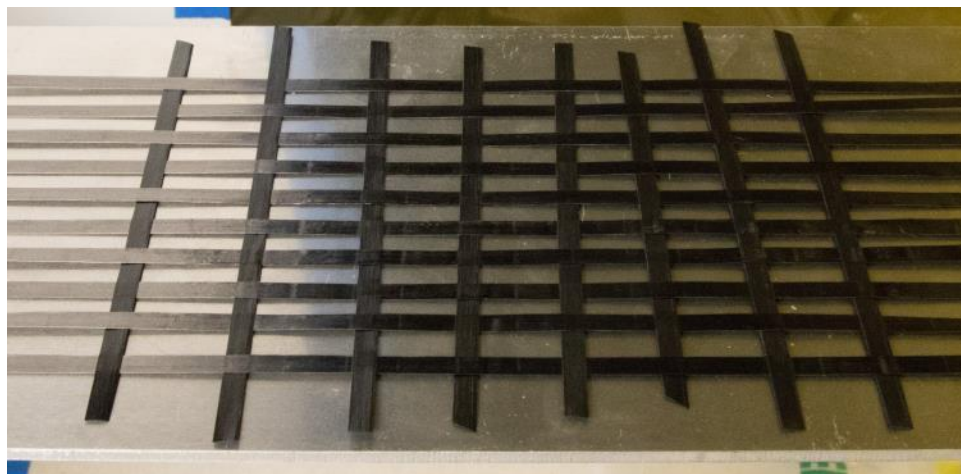


Figure 47: Finished composite lattice

Several areas for future improvement were identified during the demonstration. In particular, the prepreg feedstock that was used for this demonstration exhibited significant distortion. Whether this was due to thermal effects during the prepregging

process or if it is related to prolonged storage on the spool is unknown. Regardless of the reason, this distortion seriously complicated the weft insertion processes and required a modification of the original test plan, which was to form a composite with at least two layers. By reducing the test to a single layer, it was possible to spread the warp filaments during shedding and accommodate distortion in the filament. It will be necessary to work with our filament supplier to reduce distortion; however, an interim fix may involve heating and cooling the weft filaments prior to insertion in order to reset the thermal history.

Another issue that arose during the test was related to dwell time at the hot roller. Based on the number and size of the heaters in the warp heads and hot roller, the machine can theoretically melt 1 to 2 grams of material per second, starting with filaments at room temperature. Unfortunately, we are not currently running the rollers constantly. Instead, after each weft insertion, the warp heads move into a new position and then the roller rotates a set distance before stopping while the process repeats. This creates some locations on the warp filaments where the filament remained in the melt state longer than others, and it can even cause the filament to spread out under the pressure of the roller, resulting in uneven widths. Ongoing work is focused on decreasing the dwell time by decreasing the time required to move warp heads and insert the weft filament. At the moment, warp head speed appears to be the limiting step.

5.4 Composite Structures

The MAGIC and WEAV3D composite forming processes are noteworthy in their ability to switch between 2D and 3D woven structures on the fly. Both processes have the

ability to form traditional 2D woven geometries (plain, twill, satin); however, the 3D structures formed by these processes do not match the traditional 3D woven geometries presented in CHAPTER 2. The MAGIC and WEAV3D processes do not have designated stuffer, filling, and locking yarns, which makes them poorly suited to form homogenous 3D structures. Instead, 3D interlacing should be used as a period structure to prevent delamination propagation in larger, predominately 2D, structures.

A comparison between 2D geometries (Figure 48) and 3D geometries (Figure 49) reveals that when a 3D interlace is inserted into the 2D plain weave pattern, warp tapes are displaced to one surface of the composite, while weft tapes are displaced to the opposite surface. This results in grouping of the warp and weft tape into tape bundles. While some degree of bundling may be acceptable, too much bundling will result in excessive crimp and reduced in-plane properties. Furthermore, these bundles will be subject to increased shear stress when the composite is subjected to bending. Bundling can be reduced by using a partial 3D interlace (Figure 50), where some amount of in-plane interlacing is maintained.



Figure 48: Cross-section of 2D plain weave fabric geometry. Warp tapes (foreground and background) run from left to right. Weft tapes come out of page and are shaded black.



Figure 49: Cross-section of plain weave fabric geometry with single 3D interlace point (middle). Warp tapes (foreground and background) run from left to right. Weft tapes come out of page and are shaded black.

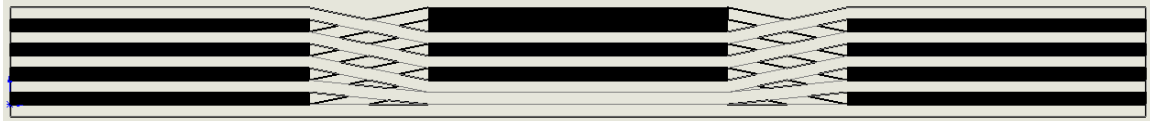


Figure 50: Cross-section of plain weave fabric geometry with partial 3D interlace point (middle). Warp tapes (foreground and background) run from left to right. Weft tapes come out of page and are shaded black.

5.5 Evaluation

The WEAV3D prototype must be evaluated in the context of the automotive global FRs and the lean manufacturing FRs. In this case, automotive FR1 (Reduce the cost of manufacturing a composite part to within 10% of a metal stamped part) and lean FRs complement each other, as any approach that addresses the lean FRs will inherently translate to reduced part cost. The fundamental difference between the MAGIC prototype and the WEAV3D prototype is the shift from batch production of composite material to flow production. By producing composite material continuously, it is possible to realize economies of scale as production volume increases, something that was not previously possible with existing composite manufacturing processes. This allows the WEAV3D prototype to satisfy both lean FR3 (Flow production should be maximized) and automotive FR1. Furthermore, constraint 1 (Minimum annual production rate of 250,000 parts) is indirectly addressed through the fulfilment of automotive FR1 and lean FR3, as

high volume from flow production is necessary to meet the automotive cost targets. Specific cost savings are directly tied to the rate of the process steps, identified by the design parameters shown in the WEAV3D physical hierarchy (Figure 51). While most of the design parameters relate only to a single physical parameter, allowing us to satisfy Axiom 1 of Principles of Design [44], the rate of weaving is dependent on both the speed of the warp head and the speed of the weft insertion. This is because the warp heads cannot start moving to their next head position until the weft inserter finishes insertion and the weft inserter cannot start the next insertion until the warp heads are in the new head position. This is a coupled design, which violates Axiom 1; however, this problem is inherent to the weaving process, so it is difficult to envision a solution that would successfully decouple this design parameter.

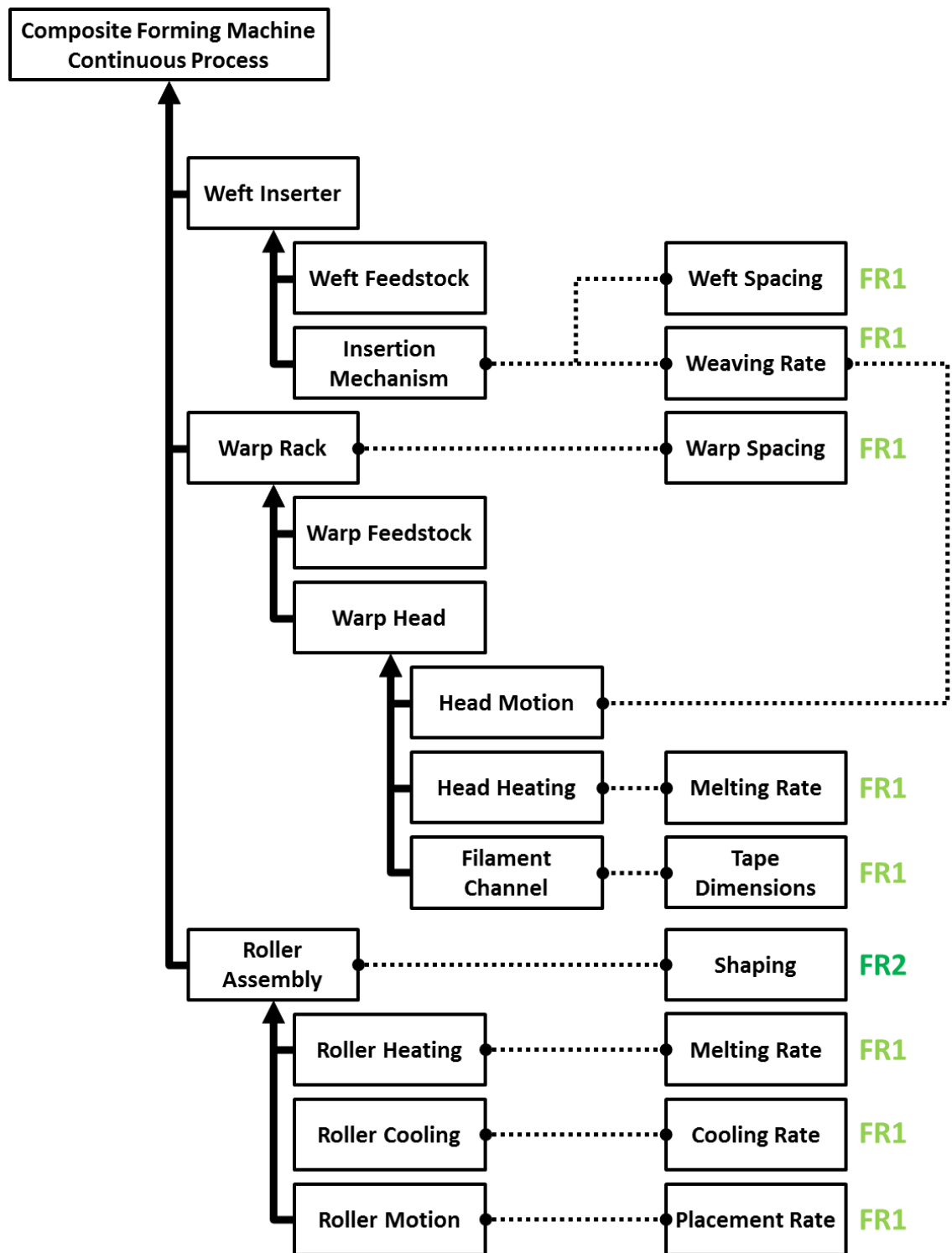


Figure 51: WEAV3D Physical Hierarchy and Design Parameters

Automotive FR2 (Reduce the number of parts through part integration) and lean FR1 (Material waste should be minimized or reused within the manufacturing process) are also complementary in this design. The WEAV3D prototype is not as material-efficient as the MAGIC prototype during the composite formation process. This is because the WEAV3D system is unable to cut filaments during the formation step and is also unable to rotate between layers. This necessitates a trim step that may result in significant trimming waste, depending on part orientation. To satisfy lean FR1, we can propose a hypothetical shaping step that occurs after the formation of composite lattices. This shaping step involves grinding or chopping the composite trim waste and then over-molding the composite lattice using LFT compression molding. Over-molding fills the gaps in the structural lattice, which enables precise control of surface finish and part thickness. This also allows us to satisfy automotive FR2, which requires part integration. During over-molding, it is possible to integrate wiring clips, ducting, and stand-offs directly into the composite panel. The WEAV3D process can be directly integrated with existing LFT forming lines, to allow flow production from composite feedstock, through to the final part. This allows us to fulfill lean FR2 (Inventory steps should be minimized), in conjunction with the inventory management benefits that were previously described for the MAGIC prototype.

In summary, the WEAV3D prototype successfully demonstrates that it can fulfill all of the automotive and lean functional requirements, albeit with some coupling at lower levels of the FR hierarchy.

CHAPTER 6. MODELLING OF COMPOSITE PROPERTIES

This chapter describes a computational model that is intended to be used in conjunction with the WEAV3D machine to aide in the design of structurally optimized composites.

6.1 Concept

Most commercially available composite models focus on fiber type, fiber orientation, fiber volume fraction, and weave pattern in each layer. This approach makes sense given that most manufacturing methods are limited to depositing one layer at a time. These methods also utilize homogeneous fabric structures for each ply. If a composite is desired that combines a satin-weave carbon fabric with a plain-weave aramid fabric, it would be necessary to cut separate plies of each material and then stack them together to form the laminate. The MAGIC and WEAV3D composite manufacturing methods allow for variation of fabric geometry (2D and 3D), reinforcement fiber, and fabric density within a given layer of the composite. This dramatically increases the size of the design space, as an optimization program would need to sweep a very large number of possible variables. As this is currently not available from commercial computer models, we sought to develop a modelling program that could be used to generate structures specifically designed to be produced using the WEAV3D machine.

Our modelling approach was conceived as an attempt to reduce the computational complexity of the finite element model by using analytical methods to simplify the

internal geometry into regular volume elements. As discussed in the literature review, finite element models require a precise geometric representation of the composite as part of model preprocessing. This makes automated model generation difficult, particularly if the model is intended to be iterated to generate optimized structures. Furthermore, if there is variation in the length scale of the geometry, computational time increases exponentially. Analytical methods excel at modelling discrete material properties, such as stiffness, averaged over a defined area; however, there are inherent limitations when using these methods to calculate stress and strain in heterogeneous structures. Our model can be described as a hybrid between the analytical fabric geometry model and a finite element approach. Each interlace point in the woven composite can be simplified into a homogenized composite tile, which can be assembled into a finite element model. A hybrid approach allows programmatic generation of many composite designs and reduced computational intensity.

6.2 Implementation

A test implementation of our model was developed using MATLAB R2017a (The Mathworks, Natick, MA) to leverage MATLAB's ability to handle programmatic manipulation of tensors. In order to perform the finite element analysis, we utilized MATLAB's partial differential equation (PDE) toolbox; however, this toolbox possesses some limitations which have restricted our implementation. These limitations will be discussed in further detail later in this chapter.

Our model can be divided into four components based on the functions performed in each component. A graphical representation of these four components and their

interaction with one another can be seen in Figure 52. As with most models, ours begins with a pre-processing component (Figure 52). The user defines several variables during preprocessing, including definition of the model geometry and definition of material properties. Geometry definition involves setting the outer geometry of the composite part, as well as defining the number of warp and weft yarns and the spacing between them. The model includes a list of material properties for a variety of fibers and matrix materials. The user can select from among this list or can manually enter specific properties during the pre-processing stage. The user will also input the properties of the filament that will be loaded into the WEAV3D machine, specifically the filament dimensions and fiber volume fraction.

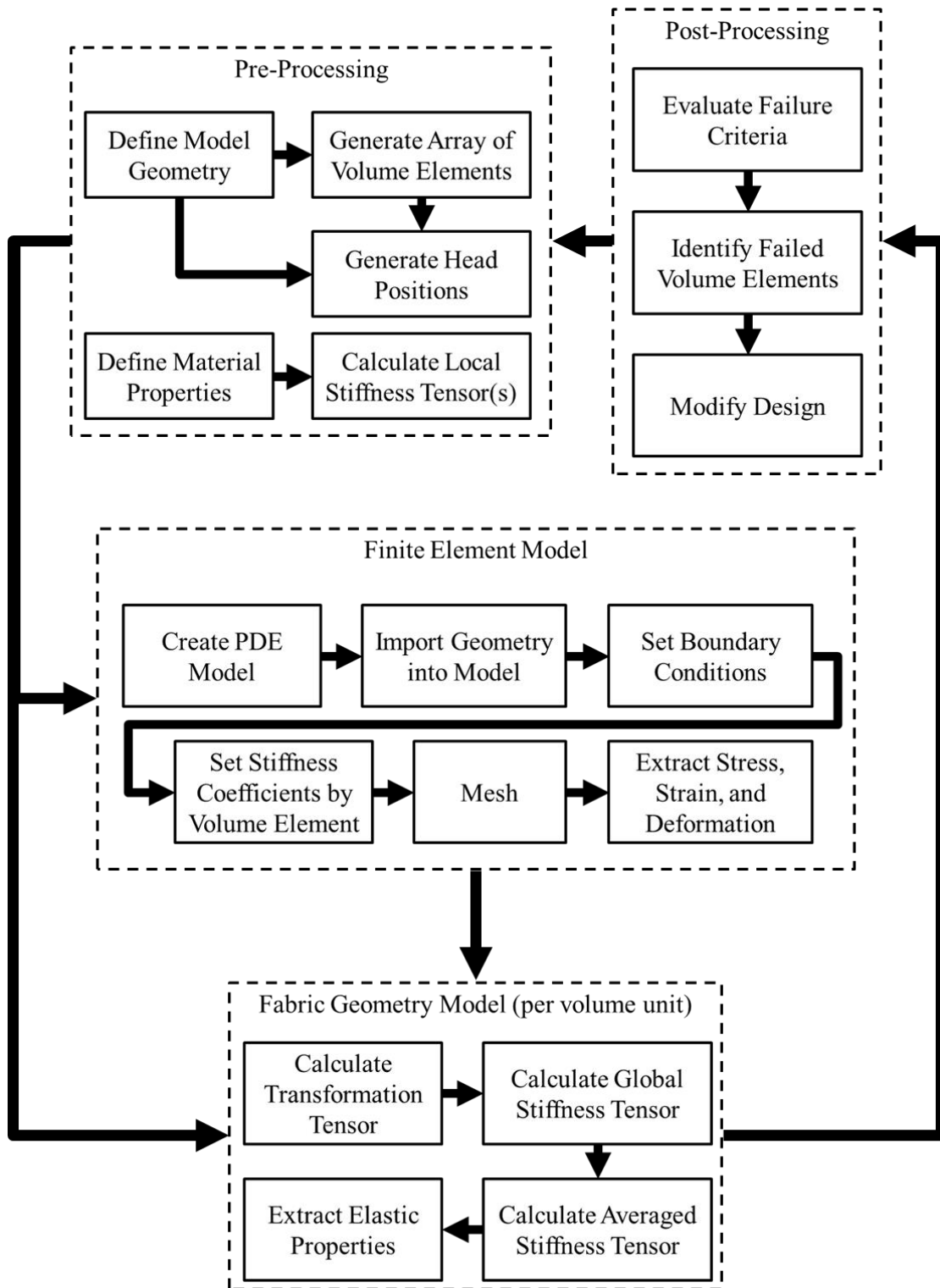


Figure 52: Illustration of how each of the four model components interact and the processes that occur within each component.

Using the user inputs, the pre-processing component then generates an array of volume elements that represent each interlace point of the fabric. This array is represented as structure array “WovenStruct” with several fields to store properties specific to each volume element. Each volume element is assumed to have a thickness equal to twice the thickness of a single filament. An example of this partition can be seen in Figure 53, which shows a 4-by-4 plain-weave fabric divided into 16 volume elements. Separately, the pre-processing component generates head positions for the WEAV3D machine. This allows the design software to send print commands to the WEAV3D machine. These head positions can be user-defined (hard-coded), or generated by the software (either randomly, or based on user-specified parameters). Each head position can be matched against a volume element and stored in WovenStruct. Figure 53 also shows the head positions generated to create a 2D plain-weave fabric. Given the limitations of the WEAV3D machine, head positions are the same for all elements that have the same X and Y position (regardless of layer number).

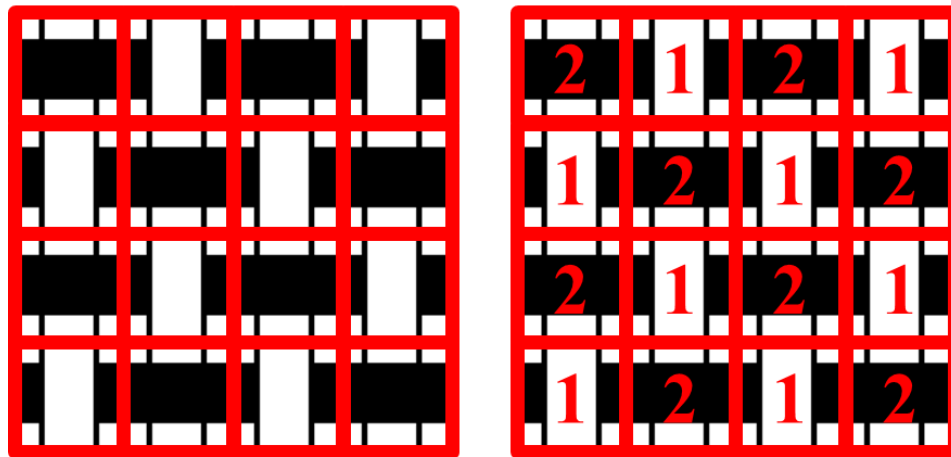


Figure 53: Woven partition (left) and head positions (right). Each red box represents a single volume element in the model.

The final task of the pre-processing component is initialization of a composite rod that represents the prepreg filament used in the machine. This step creates a stiffness tensor from the material properties that were previously defined. Additionally, the stiffness tensor for an over-molding material can be defined if the intent is to over-mold the WEAV3D preform afterwards. The pre-processing component then passes all necessary stiffness tensors and the WovenStruct variable to the fabric geometry model (FGM) component. The pre-processing component sends the geometry variable separately to the finite element analysis (FEA) component after the FGM component has finished its tasks.

The FGM reduces the weave pattern (and over-mold material) within the volume element to a homogenous, averaged stiffness tensor. The programmatic flow chart for each volume element is shown in Figure 52. Figure 54 shows four volume elements, each of which can be partitioned into at least four macro-cells to describe the crimp in the fabric: two weft cells (green) and two warp cells (blue). In the event that an open lattice structure is used, an additional cell (a combination of the four hashed cells in the volume element) will be utilized to describe empty space or over-molded material.

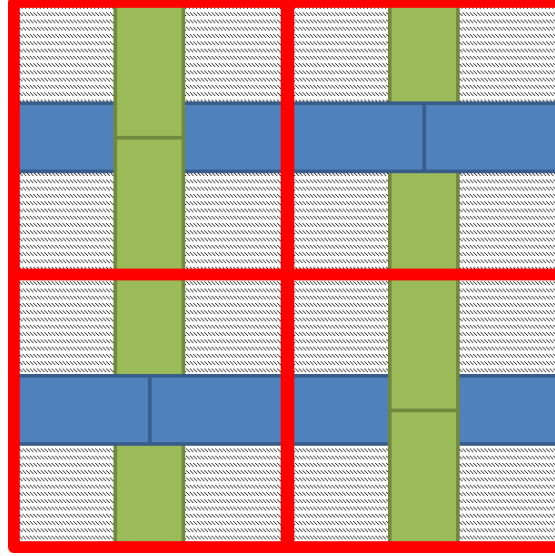


Figure 54: Macro-element partition of four volume elements. Each red box represents one volume element. Within each box, the geometry is further partitioned into two warp (blue) and two weft (green) filaments. For structures that are not fully dense, the four corners of the box (shaded regions) are either represented as empty volume or filled with reinforced plastic.

The FGM component starts by calculating the transformation tensor required for the two warp cells and two weft cells. To calculate the angle of the filament in each cell, it is necessary to reference the head position and layer number for each volume element and the elements directly adjacent. In this model, diagonal elements are not considered. In Figure 55, the cell of interest is marked with an “X”, while adjacent cells are marked A1-A4. Given that the thickness of a filament and the distance between interlace points are known, it is possible to calculate the angle based on the number of adjacent filaments that the filament of interest passes over or under. Table 3 is an example of an array that was generated to calculate the number of filaments based on head position and layer number. After the transformation tensor is calculated, the local stiffness tensor (first defined in the pre-process) is transformed into the global stiffness tensor. This process is repeated for each macro-cell, before the macro-cells are averaged to generate a single

stiffness tensor that represents the entire volume element. Finally, the elastic properties (E11, E22, E33, etc.) are extracted from the stiffness tensor. Both the global stiffness tensor and the elastic properties are stored in WovenStruct. After WovenStruct has been updated for all volume elements, WovenStruct is sent to the FEA component.

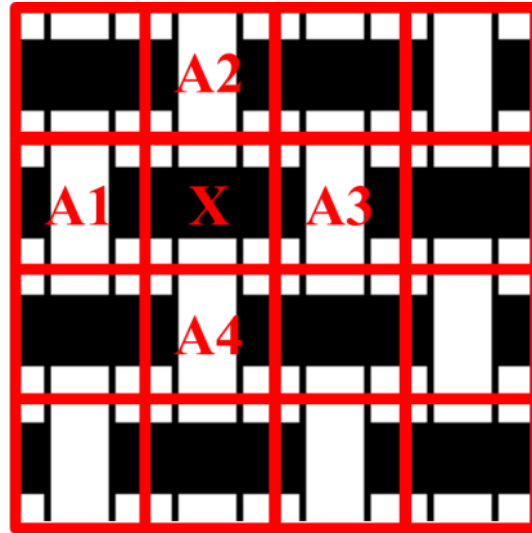


Figure 55: Cell of interest is marked with an “X”. Adjacent cells are labeled “A1” through “A4”

Table 3: Print head position conversion table

		Layer 1				Layer 2				Layer 3				Layer 4			
		To				To				To				To			
		1	2	3	4	1	2	3	4	1	2	3	4	1	2	3	4
Form	1	0	1	1	1	0	1	2	2	0	1	2	3	0	1	2	3
	2	-1	0	0	0	-1	0	1	1	-1	0	1	2	-1	0	1	2
	3	-1	0	0	0	-2	-1	0	0	-2	-1	0	1	-2	-1	0	1
	4	-1	0	0	0	-2	-1	0	0	-3	-2	-1	0	-3	-2	-1	0

The FEA component is responsible for applying load conditions to the modelled geometry in order to calculate stress and strain in each volume element (Figure 52). The component starts by instantiating a PDE model object using MATLAB's PDE toolbox and importing the geometry model created by the pre-process component. At the time of writing, MATLAB is only able to handle multiple volumes with different stiffness properties in its 2D PDE toolbox. As such, we have been forced to reduce our FEA model from 3D to 2.5D. Boundary conditions are set such that one edge of the composite is a fixed boundary (zero deformation permitted) and one edge has an applied stress. The remaining edges are free surfaces. To represent the 2.5D condition, the applied stress is calculated based on the actual thickness of the composite.

The next step in the FEA process is to set the stiffness coefficient for each volume element. To work around the 2D restriction, we averaged the stiffness tensor through the thickness of the composite. This means that for a four-layer composite, the FEA element at position (1,1) will be the average of volume elements in positions (1,1,1), (1,1,2), (1,1,3), and (1,1,4). We believe that this results in an approximate representation of the laminate stiffness, given the low thickness of each layer. After the layers have been averaged, the PDE coefficients (stiffness, body forces, etc.) are set for that particular volume element. This process is repeated for each volume element before the entire geometry is meshed. Mesh size and "jiggle" iterations are set to ensure that each volume element has the same mesh pattern. Matlab uses the *jiggle* function to optimize mesh size and pattern, and with sufficient *jiggle* iterations it is possible to ensure that every volume element has the same mesh pattern. At this stage, the finite element model can be

executed and the results can be captured. Using these results, it is possible to calculate stress and strain in each volume element and store these values in WovenStruct.

The final step in the model is the post-processing component (Figure 52). This component is responsible for applying failure criteria to the results from the FEA. While a number of failure methods can be used, we elected to use the Max Strain condition for the sake of simplicity in our representative implementation. If no elements are identified as failing, the model is finished and the head positions can be extracted from WovenStruct and sent to the WEAV3D machine for production. If one or more volume elements are identified as failing, the user or the post-process component can trigger design iterations until the failure criteria are satisfied. The current implementation of the model visually flags failed volume elements to allow the user to re-run the model with different parameters (increased weave density, additional layers, different weave patterns, etc.).

6.3 Validation

Validation of the model focused on independently validating the FGM component and FEA components, as well as demonstrating the ability of the post-processing component to flag failed cells. The FGM model has already been well validated for describing repeating unit cells; however, our implementation treats each interlace point as a separate cell, so it is important to show that our approach is equivalent. The material properties used for the validation are based on AS4 carbon fiber and PEKK resin, with a 60% fiber volume fraction. For the purpose of validation, we generated cells that are fully

filled by woven filament (i.e., no over-mold). The geometry selected for this validation model was 10 warp filaments by 10 weft filaments with filament spacing of 10 mm.

Using the preprocessing component, we can generate the 2D geometric representation of the woven volume elements (Figure 56). For the purpose of validation, we elected to use a repeating plain-weave fabric geometry (alternative head positions of 1 and 2). This will allow us to validate the stiffness of each volume element by comparing the data against pre-existing fabric geometry models that describe the repeat units of the plain-weave geometry (two warp and two weft filaments).

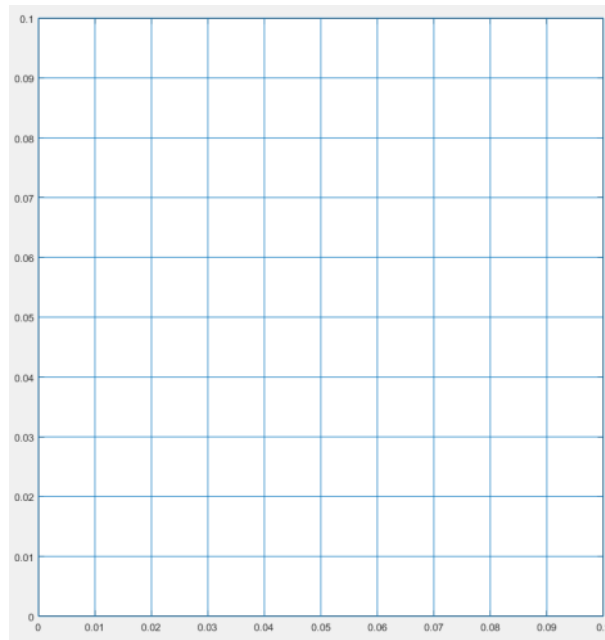


Figure 56: 2D geometric representation of volume elements. Each blue square represents one 10 mm by 10 mm element.

After generating head positions and setting initial variables, the FGM component is instantiated to calculate the stiffness tensors in each volume element. Table 4 shows a comparison of elastic moduli between a plain-weave fabric calculated in a traditional

fabric geometry model and one calculated using the volume element FGM model. It can be seen from the table that there is a deviation between the elastic moduli, which is largely due to the difference in crimp angle between the two models. The traditional FGM model assumes a “jammed” fabric with a high number of picks per inch. This results in an approximate crimp angle of 6 degrees. On the other hand, the volume element FGM model is based on the physical limitations of the WEAV3D machine. As such, there are fewer picks per inch, but each filament is considerably wider than one that would be used in a traditional fabric. This results in a much lower crimp angle of 1.15 degrees. Due to the low crimp angle, more of the fiber lays in the plane of the composite, which increases the in-plane properties (E11, E22, G12) and decreases the out-of-plane properties (E33, G23, G13) when compared to the traditional FGM plain weave.

Table 4: Comparison of moduli of traditional FGM and Volume Element FGM. Calculations for both models were performed using MATLAB.

		Traditional FGM (Plain Weave)	Volume Element FGM Model (Plain Weave)	Deviation
Tensile	E11	68 GPa	70 GPa	2.55%
	E22	68 GPa	70 GPa	2.55%
	E33	7.1 GPa	7 GPa	-0.84%
Shear	G23	4.6 GPa	4 GPa	-13.29%
	G13	4.6 GPa	4 GPa	-13.29%
	G12	5.8 GPa	5.8 GPa	0.61%

Once the stiffness tensors have been generated for each volume element, the array containing the stiffness tensors is passed to the FEA component. The FEA component also receives the geometry model from the handler, which is used to instantiate the finite element model. Due to the aforementioned 2D limitations of the MATLAB partial differential equations toolbox, we elected to set $N=2$. After instantiating the model, it is necessary to set the boundary conditions. Figure 57 shows a free body diagram of the load that was used for this validation. Translating the free body diagram into FEA boundary conditions, the fixed left edge of the composite plate is represented with a Dirichlet boundary condition equal to zero. The 10 kN load applied to the right-most edge of the lower right volume element is represented as a Neumann boundary condition that is set to 5 GPa ($10 \text{ kN}/(0.2 \text{ mm} \times 10 \text{ mm})$). The remaining edges are set to be “free” boundaries, allowed to deform under load.

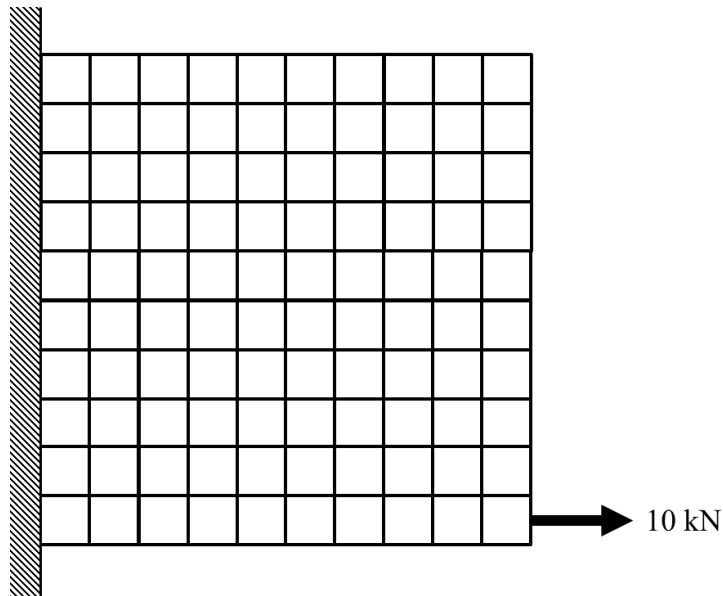


Figure 57: Free body diagram of boundary conditions. A 10 kN point load is applied to the lower-right volume element. It is assumed that the left side of the composite is fixed, while all remaining surfaces are free.

After boundary conditions have been set, PDE variables are set as described above. The geometry model is meshed before the FEA model is solved and the results are saved to the structure array. These results include the strain and stress for each volume element. Figure 58 shows the deformed mesh after the model has been solved.

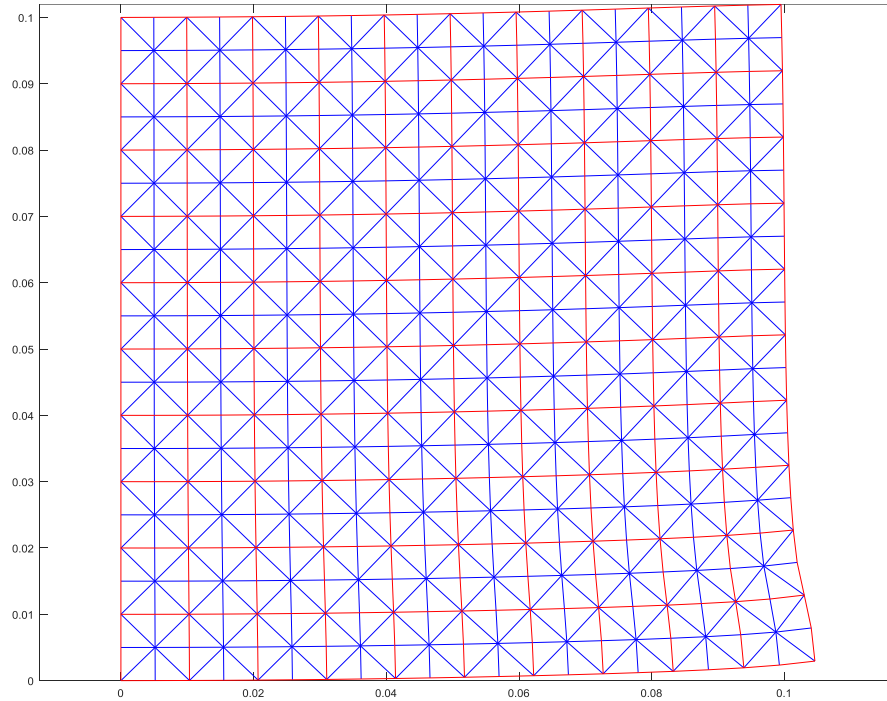


Figure 58: Deformed mesh after FEA analysis. The red boxes represent each volume element in the model, while the blue triangles show the mesh used for this test.

Finally, the post-processing component is used to evaluate the strain against the max strain failure condition (0.021 for AS4 carbon fiber). Failing volume elements are flagged by the post-processing component so that the user can change the composite parameters in subsequent iterations of the design. Figure 59 shows a graphical representation of the volume elements that were flagged for this FEA model. It can be seen from the deformed mesh, that the lower rows of the composite are subject to a large tensile deformation; however, the post-processing component has also flagged the top

right corner of the composite as exceeding the max strain criterion. Because of the point load, a large tense strain occurs in the bottom rows, while the top corner experiences some compressive effects due to the fixed boundary on the left side.

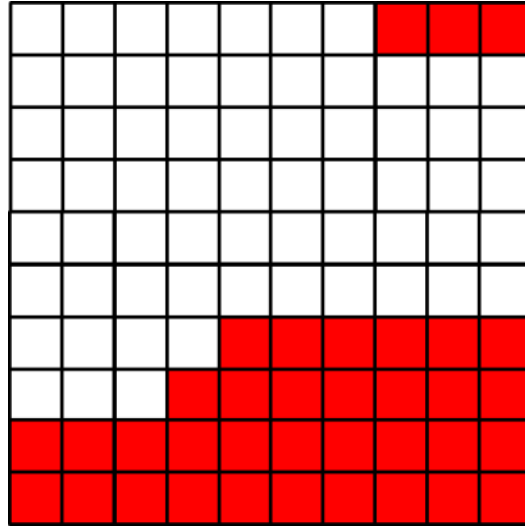


Figure 59: Graphical representation of flagged volume elements. A filled red box indicates that a particular volume element has exceeded the predetermined failure condition, in this case, the max strain parameter.

This example serves to demonstrate the three conditions that were required for successful validation of the hybrid FGM/FEA model: the volume element FGM approach and the traditional fabric geometry model predict similar stiffness tensors, the FEA component is able to model an assembly of volume elements with different stiffnesses, and the post-processing component is capable of flagging volume elements that fail the preset failure criteria.

CHAPTER 7. CONTRIBUTIONS AND FUTURE WORK

7.1 Contributions

A method of design that combines a top-down definition of functional requirements with a bottom-up approach through the use of elementary steps was developed to address the composite material needs of the aerospace and automotive industries, while also integrating lean manufacturing into the total composite value chain. The case studies presented deal specifically with how this methodology can be applied to develop novel composite forming processes; however, composites are not the only field where this approach may be useful. By understanding both the high-level needs of a process and the fundamental process steps, and relating them through the use of design parameters, any number of existing processes may be optimized or replaced with more efficient alternatives. This is particularly true for processes which currently rely on a long supply chain and where batch processing is currently preventing the process from reaching economies of scale.

This work resulted in the filing of two non-provisional patent applications. The first patent application, U.S. No. 14/821,502, was filed on August 8, 2015, and claims priority to a U.S. provisional application filed one year prior. This patent application describes the MAGIC composite forming machine, and includes claims covering the composite forming method, the composite forming machine, and a composite product consisting of multiple woven geometries within a single layer and the ability to combine multiple layers. Following restriction, Georgia Tech elected to initially pursue the method claims. A notice of allowance for these claims has been received, and the patent is expected to

issue in the 2017 calendar year. We expect this application to result in a total of three patents, based on the initial restriction and future divisional filings. The second patent application, PCT/US 2017/032703, was filed on May 15, 2017, and cites priority to a U.S. provisional application filed one year earlier. This application includes claims covering two machine embodiments (one of which is the model for the WEAV3D bench-scale prototype) and the method used by these machines to form a composite product. This patent application will likely result in two-to-three issued patents after restriction and divisional filings.

Georgia Tech used independent consultants to conduct a patentability search prior to filing both patents and did not find any similar technologies. Therefore, we believe both inventions to be novel and non-obvious. In addition, a preliminary freedom-to-operate (FTO) search was conducted as part of a commercialization course at Georgia Tech. This FTO search did not identify any significant barriers to practicing the invention.

Beyond the intellectual contributions of this work, there is also a societal contribution that should be mentioned. As described in the introduction, there is a global push to reduce CO₂ emissions through the reduction of fuel consumption in the transportation industry. Composite materials have long offered the promise of improved fuel economy through weight reduction; however, basic economics have limited the ability of designers to realize these benefits. While focusing on reducing the cost of raw materials, particularly of carbon fiber, will solve some of the issues preventing development of cost-effective composites, this is only half of the equation. Composite materials are inherently linked to the manufacturing processes that produce them and too

often, engineers try to adapt existing processes when applying composites to new applications. The WEAV3D composite forming machine offers a novel approach to the problem of mass production of composites, and may serve as a template for bringing composite materials to cost-sensitive industries in a scalable manner.

7.2 Future Work

The bench-scale model was sufficient to demonstrate the technical potential of the WEAV3D composite forming machine; however, this prototype is currently limited to forming test coupons and processing samples due to the narrow warp rack. For automotive applications, we anticipate a minimum warp rack width of 1 m, with a preferred width of 2 m. At this scale, it would be possible to produce full-scale sample parts that could be utilized in component tests and limited production. Efforts are being made to secure funding required for machine scale-up, with the goal of completing a full-scale prototype by mid-late 2018. In addition to scale-up, efforts will also focus on improving the linear speed of fabrication. Potential bottlenecks include warp head positioning speed, weft insertion rate, roller drive speed, and heat transfer limits in both the warp heads and roller assembly. Using the existing bench-scale prototype, we intend to evaluate the limits of each subsystem, to identify which subsystems should be prioritized for redesign.

Beyond machine improvements, work should also be done to demonstrate how this process can integrate with existing processes to produce end-use parts. Future research will need to study how the lattice structures produced by the WEAV3D machine can be integrated with long-fiber thermoplastic compression molding and/or injection molding.

Both processes would benefit from the addition of a load-bearing structural lattice and would compensate for WEAV3D's inability to form fully dense parts in its current embodiment. Preliminary work has demonstrated that integrating WEAV3D lattice structures with injection molding is technically feasible (Figure 60); however, further research is required to characterize the properties of these hybrid materials. Additional research efforts should also assess the feasibility of laminating the structural lattice to the sheet molding compound during the WEAV3D composite forming process by utilizing the same hot rollers that consolidate the composite.

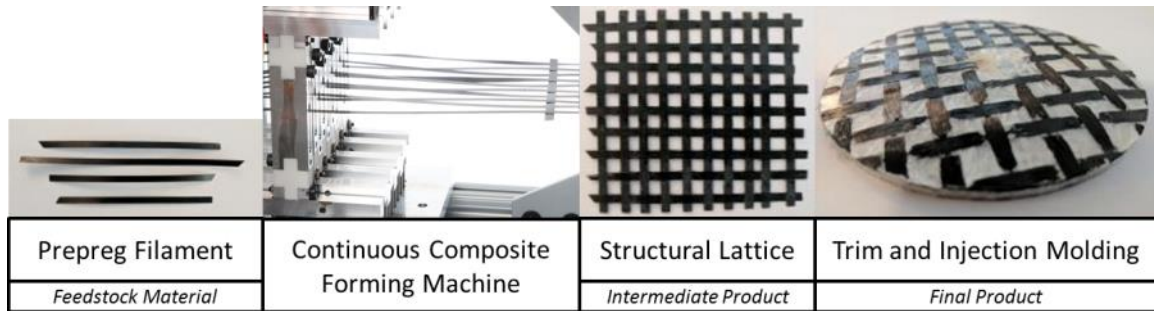


Figure 60: Proposed WEAV3D-injection molding process chain

While development of the WEAV3D machine was prioritized due to limited resources, the MAGIC machine has several features that may make it more appealing for certain applications in the future. The MAGIC machine has much greater control than the WEAV3D machine over individual filament deposition and filament alignment, which may make MAGIC more appealing to industries that require highly optimized structures. Future work on the MAGIC machine should start by redesigning many of the subsystems in light of the lessons from WEAV3D. For example, the WEAV3D weft inserter is mechanically simpler than the one developed for the MAGIC prototype and the WEAV3D motion system is substantially more durable.

Future work on the composite optimization model will entail overcoming several challenges, some of which are directly tied to the MATLAB programming language. We anticipate future versions of MATLAB to have the ability to set different stiffness values for 3D volume elements, but there is no specific timeline for this implementation. As an alternative, future implementations of the model could utilize the MATLAB Simulink tool to export the pre-processing and FGM components into COMSOL Multiphysics (COMSOL, Stockholm, Sweden) for finite element analysis. The FEA results would then be reimported into MATLAB for post-processing. This implementation would be substantially more complex than a pure MATLAB implementation, due to the idiosyncrasies of passing model and volume element data between MATLAB and COMSOL. A third alternative would be to build the model entirely in a dedicated, engineering-grade FEA program such as ANSYS Multiphysics (ANSYS, Cannonsburg, PA). This would likely solve the issues with the FEA component, but may introduce additional issues with the FGM component.

A commercial-grade implementation of the model would require the development of a user-friendly graphical user interface and complete automation of the optimization process (within user-defined boundaries). Furthermore, the commercial-grade implementation would need to be able to model complex, curvilinear panels with irregular edges. This is well beyond the scope of the current implementation and may represent a significant programming challenge.

7.3 Commercialization

Efforts are ongoing to commercialize the WEAV3D technology. In the past year, over 140 customer discovery interviews were conducted to identify potential customers and to find the best product-market fit based on the value propositions of the WEAV3D machine. Based on these interviews, we have decided to pursue the automotive industry as our initial target market. This industry has a strong desire to adopt carbon fiber composites due to a combination of regulatory and competitive pressures relating to fuel economy, but current composite forming methods are unable to meet industry cost and rate targets needed for wide adoption. We believe that WEAV3D has the potential to meet these targets.

In addition to customer discovery, I have also completed a Doctoral Minor in Technology Commercialization. As part of this two-year program, a multidisciplinary team consisting of myself, two Emory Law students, and two Georgia Tech MBA students developed a commercialization strategy and business plan for bringing the WEAV3D technology to market. Using this business plan, we competed at several collegiate entrepreneurship competitions across the United States, taking 1st place at the MegaWatt Venture Championship, 1st place at the TiE Atlanta Young Entrepreneur's Competition, 2nd place at the Georgia Bowl Business Plan Competition, and 3rd place at the Cleantech University Prize competition. It is my intention to found a startup company to bring the WEAV3D technology out of the laboratory and into the market.

REFERENCES

- [1] Wikipedia Contributors. (2017, Nov 18, 2014). *Micarta* - *Wikipedia*. Available: <https://en.wikipedia.org/wiki/Micarta>
- [2] L. Tong, A. P. Mouritz, and M. K. Bannister, "Chapter 1 - Introduction," in *3D Fibre Reinforced Polymer Composites*, L. T. P. M. K. Bannister, Ed., ed Oxford: Elsevier Science, 2002, pp. 1-12.
- [3] A. International, "Standard Terminology for Additive Manufacturing Technologies (Withdrawn 2015)," vol. ASTM F2792-12a, ed. West Conshohocken, PA: ASTM International, 2012.
- [4] C. Hull, "Apparatus for production of three-dimensional objects by stereolithography," United States Patent, 1986.
- [5] S. Crump, "Apparatus and method for creating three-dimensional objects," United States Patent, 1992.
- [6] I. Gibson, D. W. Rosen, and B. Stucker, *Additive manufacturing technologies : rapid prototyping to direct digital manufacturing*. London ; New York: Springer, 2010.
- [7] C. Deckard, "Method and apparatus for producing parts by selective sintering," United States Patent, 1989.
- [8] J. L. Ahmed Arabi Hassen, Xun Chen, Brian Post, Lonnie Love, Vlastimil Kunc, "Additive Manufacturing of Composite Tooling Using High Temperature Thermoplastic Materials," *SAMPE 2016 Conference Publication*, May 26, 2017 2016.
- [9] Markforged. (November 20, 2014). *The World's First Carbon Fiber Printer 3D Printer*. Available: www.markforged.com
- [10] F. v. d. K. Yoichiro Koga, Akira Todoroki, Masahito Ueda, Yoshiyasu Hirano, Ryosuke Matsuzaki, "The Printing Process Of 3D Printer for Continuous CFRTP," *SAMPE 2016 Conference Publication*, May 26, 2016 2016.
- [11] E. Dictionary. (2017). *Composite Material*. Available: <http://www.engineering-dictionary.com/index.php?definition=962#>
- [12] D. Hull and T. W. Clyne, *An introduction to composite materials*, 2nd ed. Cambridge ; New York: Cambridge University Press, 1996.

- [13] V. K. Ganesh, S. Ramakrishna, S. H. Teoh, and N. K. Naik, "Microstructural design of textile composites," *Materials & Design*, vol. 18, pp. 175-181, 10/1/ 1997.
- [14] J. M. B.K. Behara, Rajesh Mishra, and Dana Kremenakova, "Modeling of Woven Fabrics Geometry and Properties," *Woven Fabrics*, 2012.
- [15] S. Adanur, *Wellington Sears Handbook of Industrial Textiles*. Lancaster, Pa.: Technomic Pub., 1995.
- [16] C. Oberste, B. Wang, K. Wang, "Interlaced three-dimensional printed composites and method for fabricating the same," United States Patent, 2016.
- [17] L. Tong, A. P. Mouritz, and M. K. Bannister, "Chapter 2 - Manufacture of 3D Fibre Preforms," in *3D Fibre Reinforced Polymer Composites*, L. T. P. M. K. Bannister, Ed., ed Oxford: Elsevier Science, 2002, pp. 13-46.
- [18] M. McClain, J. Goering, "Overview of Recent Development in 3D Structures," *SME Composites Manufacturing*; pp. 1-12 2012.
- [19] A. Kollmannsberger. November 19, 2014). Automated Fiber Placement. *Lehrstuhl Fur Carbon Composites*.
- [20] Molded Fiber Glass Companies (November 19 2014). *Resin Transfer Molding Process*.
- [21] Molded Fiber Glass Companies (November 19 2014). *Compression Molding Process/SMC*.
- [22] T. Ishikawa and T. W. Chou, "One-dimensional micromechanical analysis of woven fabric composites," *AIAA Journal*, vol. 21, pp. 1714-21, 12/ 1983.
- [23] T. Ishikawa and T. W. Chou, "Stiffness and strength behaviour of woven fabric composites," *Journal of Materials Science*, vol. 17, pp. 3211-20, 11/ 1982.
- [24] T. Ishikawa and C. Tsu-Wei, "Nonlinear behavior of woven fabric composites," *Journal of Composite Materials*, vol. 17, pp. 399-413, 1983.
- [25] T. Ishikawa, M. Matsushima, Y. Hayashi, and T. W. Chou, "Experimental confirmation of the theory of elastic moduli of fabric composites," *Journal of Composite Materials*, vol. 19, pp. 443-58, 1985.
- [26] N. K. Naik and P. S. Shembekar, "Elastic behavior of woven fabric composites. I. Lamina analysis," *Journal of Composite Materials*, vol. 26, pp. 2196-225, / 1992.
- [27] N. K. Naik and P. S. Shembekar, "Elastic behavior of woven fabric composites. III. Laminate design," *Journal of Composite Materials*, vol. 26, pp. 2522-41, / 1992.

- [28] P. S. Shembekar and N. K. Naik, "Elastic behavior of woven fabric composites. II. Laminate analysis," *Journal of Composite Materials*, vol. 26, pp. 2226-46, / 1992.
- [29] Y. A. Gawayed, C. Pastore, and C. S. Howarth, "Modification and application of a unit cell continuum model to predict the elastic properties of textile composites," *Composites Part A (Applied Science and Manufacturing)*, vol. 27A, pp. 149-55, / 1996.
- [30] P. Tan, L. Tong, and G. P. Steven, "Models for predicting thermomechanical properties of three-dimensional orthogonal woven composites," *Journal of Reinforced Plastics and Composites*, vol. 18, pp. 151-85, / 1999.
- [31] P. Vandeurzen, J. Ivens, and I. Verpoest, "A three-dimensional micromechanical analysis of woven-fabric composites. I. Geometric analysis," *Composites Science and Technology*, vol. 56, pp. 1303-15, / 1996.
- [32] P. Vandeurzen, J. Ivens, and I. Verpoest, "A three-dimensional micromechanical analysis of woven-fabric composites. II. Elastic analysis," *Composites Science and Technology*, vol. 56, pp. 1317-27, / 1996.
- [33] P. Vandeurzen, J. Ivens, and I. Verpoest, "Micro-stress analysis of woven fabric composites by multilevel decomposition," *Journal of Composite Materials*, vol. 32, pp. 623-63, / 1998.
- [34] J. Xu, B. N. Cox, M. A. McGlockton, and W. C. Carter, "A binary model of textile composites—II. The elastic regime," *Acta Metallurgica et Materialia*, vol. 43, pp. 3511-3524, 9// 1995.
- [35] F. Stig and S. Hallström, "Influence of crimp on 3D-woven fibre reinforced composites," *Composite Structures*, vol. 95, pp. 114-122, 2013.
- [36] J. D. Whitcomb, "Iterative global/local finite element analysis," *Computers and Structures*, vol. 40, pp. 1027-31, / 1991.
- [37] K. Woo and J. Whitcomb, "Global/Local Finite Element Analysis for Textile Composites," *Journal of Composite Materials*, vol. 28, pp. 1305-1321, 1994.
- [38] F. Stig and S. Hallström, "A modelling framework for composites containing 3D reinforcement," *Composite Structures*, vol. 94, pp. 2895-2901, 2012.
- [39] R. Hill, "Theory of mechanical properties of fibre-strengthened materials. I. Elastic behaviour," *Journal of the Mechanics and Physics of Solids*, vol. 12, pp. 199-212, 1964.
- [40] R. Hill, "Theory of mechanical properties of fibre-strengthened materials. II. Inelastic behaviour," *Journal of the Mechanics and Physics of Solids*, vol. 12, pp. 213-219, 1964.

- [41] S. W. Tsai and E. M. Wu, "A General Theory of Strength for Anisotropic Materials," *Journal of Composite Materials*, vol. 5, pp. 58-80, 01/ 1971.
- [42] A. N. B. R. Sundar, R.M. Satheesh Kumar, "A Review on Lean Manufacturing Implementation Techniques," *Procedia Engineering*, vol. 97, pp. 1875-1885, 2014.
- [43] Z. Tadmor, "Machine Inventions, Innovation, and Elementary Steps," *Advances in Polymer Technology*, vol. 21, pp. 87-97, 2002.
- [44] N. P. Suh, *The Principles of Design*. New York: Oxford University Press, 1990.